

This section presents a framework for the flood risk analysis and also presents a brief discussion on flood vulnerability analysis and results. The flood vulnerability of the Delta and Suisun Marsh levees were assessed for a series of flood scenarios. More detailed information on levee vulnerability analysis is presented in the Levee Vulnerability Technical Memorandum. For each flood scenario, the corresponding flood stage was computed using the hydrological model developed for the site. Each flood scenario was defined using a parameter, daily Total Delta Inflow (TDI), in cfs. The frequency of major flood inflows, the patterns of inflows from the various rivers, and Delta water surface elevations associated with these flows are all critical in determining flood risk.

7.1 DELTA INFLOW

Average daily inflows into the Delta are available from the DWR website for the 50 water years (WYs) from October 1, 1955, through September 30, 2005 (WYs 1956 through 2005). These data include average daily inflows for all major streams entering the Delta and the total inflow into the Delta (DWR 2006). The major streams or stream groups included in the dataset are Sacramento River, Yolo Bypass, Cosumnes River, Mokelumne River, San Joaquin River, and miscellaneous streams. Flows in miscellaneous streams are primarily Calaveras River flows. The locations of the stations used in the analysis are shown on Figure 7-1. Measured average daily inflows into the Delta are summarized graphically on Figure 7-2. Figure 7-2a presents total inflows into the Delta for the period of record. Figure 7-2b presents inflows from Sacramento River and Yolo Bypass, the major contributors to total inflow (>80 percent). Figure 7-2c presents inflows from San Joaquin River, the third-largest contributor to total inflow (~10 percent).

One of the objectives of these studies is to develop estimates of hydrologic characteristics of the Delta under current conditions in the tributary watersheds. Thus, it was necessary to examine the available Delta inflow data to determine if these data adequately reflect current watershed conditions or if the statistical characteristics of the data have significantly changed during the period of recorded data due to new reservoirs in the watersheds, developments in the watershed, land use changes, and other factors.

As shown on Figure 7-2, the period from about 1987 to 1993 had relatively fewer large flood inflow events than before 1987. This 6-year period had below-average precipitation and is the longest period of below-average rainfall between 1955 and 2005. This pattern suggests that during the 50-year period of record, more drought years occurred in the recent period of record than in earlier years. It is therefore desirable to use the entire period of available inflow record to avoid or reduce any statistical bias caused by the recent drought years.

Several dams and reservoirs, developments, and other changes have been constructed in the watersheds tributary to the Delta, and the impacts of these changes on inflows into the Delta were reviewed in the DRMS studies. Construction of new dams and reservoirs in the tributary watersheds could be a large contributor to changes in characteristics of runoff to the Delta. However, as discussed in the following paragraphs, it is believed that changes related to reservoirs and watershed developments are associated with water supply and environmental flow releases from the reservoirs and have minimal impact on flood inflows into the Delta.

Table 7-1 is a partial list of dams and reservoirs that have been constructed in the tributary watersheds. As shown in Table 7-1, the reservoirs behind Oroville and New Melones dams are two of the largest reservoirs constructed during the period of available inflow measurements.

Analyses were made to determine if Oroville Dam and other watershed changes since construction of the dam had a significant impact on Delta inflows from Sacramento River and Yolo Bypass. Similar analyses were made with regard to San Joaquin River since construction of New Melones Dam.

Table 7-2 summarizes the measured Delta inflows for three periods. For the Sacramento watershed, the periods are the pre-Oroville Dam period (1956–1968), the post-Oroville Dam period (1969–2005), and the entire period of record. For the San Joaquin River watershed, the periods are the pre- and post-New Melones Dam periods (1956–1979 and 1980–2005, respectively), and the entire period of record. Since no major storage projects have been developed on the Delta tributaries since construction of New Melones Dam, the post-New Melones Dam period is considered to represent current conditions. As shown in Table 7-2, the average number of days per year with high Delta inflows (>100,000 cfs) from San Joaquin River is greater during current conditions in the watershed than before New Melones Dam was constructed, and the average number of days per year of low Delta inflows (<100,000 cfs) is less. This situation is contrary to what would be expected if New Melones Dam and reservoir had a significant impact on flood inflows. Similarly, Table 7-2 shows more high (>100,000 cfs) and fewer low (<100,000 cfs) total inflows into the Delta from the Sacramento River watershed since the construction of Oroville Dam.

Table 7-3 lists, in descending order, the maximum daily TDI for each WY of the period of record. Examination of the flood inflow dates presented in Table 7-3 show that 4 out of the 5 largest inflow days and 7 out of the 12 largest inflow days occurred after 1979, after construction of Oroville and New Melones dams. A review of the maximum daily inflow data for San Joaquin River shows similar results: three of the five largest single-day inflows have occurred since 1979, and 7 of the 10 largest have occurred since 1979. The data in Table 7-3 also show no general trends in increasing or decreasing runoff to the Delta. Of the largest 25 inflows, 12 occurred during the most recent 25-year period, and 13 occurred during the first half of the 50-year period of record, thereby suggesting a somewhat stationary 50-year record. Smaller peak daily inflows would be expected after the addition of reservoirs in the watersheds if the reservoirs were reducing large flows, thereby suggesting that the additional dams may not significantly reduce TDIs during major flood events. Also shown in Table 7-3 is the total volume of inflow that occurred during the peak inflow day and the 4 previous days. Although the total volume of available flood control storage in the watersheds during the flood events is not known, it is possible that runoff preceding the peak day filled whatever flood control storage was available and inflow into the reservoirs was not significantly greater than outflow on the peak day.

Another possibility is that the flood control storage provided by a new reservoir only replaces a portion of the natural floodplain storage located downstream from the dam site. This possibility could occur if under pre-dam conditions, large flood flows would overtop the channel banks and be temporarily stored on the floodplain, thereby attenuating peak inflows into the Delta. After construction of the dam, the flood flows would be temporarily stored in the reservoir, thereby attenuating the outflows and reducing or eliminating overtopping of the downstream channel banks and floodplain storage. Whether watershed storage is provided by reservoirs or the floodplain, inflows into the Delta are controlled, to some extent, by the capacity of the channels conveying runoff to the Delta.

Based on the foregoing, it does not appear that construction of reservoirs and other developments in the watersheds tributary to the Delta have a significant impact on annual peak daily Delta flood inflow characteristics during the period of record. Although it may be possible to adjust the inflow record to reflect all of the current reservoirs and watershed developments during the entire period of record, these adjustments would require significant effort and time not budgeted for these studies. Adjustment of the record would also require numerous assumptions regarding operations of the reservoirs during flood events and, most importantly, assumptions regarding levee failures and floodplain storage upstream from the Delta. These adjustments would probably incur more error than would result from using the inflow record without adjustment. For this reason and the previously discussed considerations, it is concluded that the entire period of available inflow record would be used in the hydrologic risk analyses without adjustment. It is noted that this conclusion only applies to infrequent inflow events and not nonflood inflows.

Another consideration in the DRMS studies is the season of high inflows into the Delta. It is anticipated that repairing damages in the Delta, due to any cause, will be more difficult during the high-inflow season and the repairs will likely take longer. Additionally, the possible impacts on Delta exports caused by damages may be different depending upon the time of year that the damage occurs. Thus, hydrologic characteristics in the Delta during different inflow seasons were considered in the studies. Figure 7-3 presents average daily Delta inflow versus time of the year for the period of record inflows. As shown on Figure 7-3, high inflows begin near the end of December and last to about the middle of April. Between April 15 and December 15 maximum daily inflows are less than 200,000 cfs, and most of the time maximum daily inflows are less than 100,000 cfs, with the exception of one flood that occurred during October 14–17, 1962. Thus, only two inflow seasons are considered in these studies: the high-inflow season (December 16 through April 15) and the low-inflow season (April 16 through December 15).

7.2 FLOW-FREQUENCY ANALYSIS

The magnitude of TDI for a hydrologic event of a given probability can be estimated from a frequency analysis of the measured annual peak inflow events. Table 7-4 summarizes the annual peak TDIs for each of the 50 WYs of record, the 50 high-inflow seasons in the period of record, and the 49 low-inflow seasons in the period of record.

A commonly accepted frequency distribution of hydrologic events is the Log Pearson Type III (LPIII) distribution. This frequency distribution is recommended by the Hydrology Subcommittee of the Interagency Advisory Committee on Water Data published by the USGS (1982). LPIII uses three distribution parameters: mean, standard deviation, and skew. Annual probabilities were calculated by using the data in Table 7-4 to estimate the distribution parameters.

Results of the LPIII analyses are presented in Table 7-5 and on Figures 7-4, 7-5, and 7-6 for all WYs (all seasons), high-inflow seasons, and low-inflow seasons, respectively. The distributions of seasonal peak daily inflows into the Delta are compared to the all-seasons distribution on Figure 7-7. Table 7-6 presents the estimated parameters for each distribution.

Flood frequency as used in this risk assessment has a slightly different definition than the definition typically used in Delta flood studies. For purposes of the risk assessment, flood frequency in these studies provides a measure of the annual probability that the total inflow into the Delta will be equal or exceeded. Many different inflow patterns into the Delta can produce

any selected annual probability of occurrence, each of which could have its own set of water surface elevations in the Delta. For example, four storm events in the period of record have peak total daily inflows to the Delta that exceeded the 10-year event. For the largest storm of record, February 1986, San Joaquin River was not a significant contributor to the storm event, and Cosumnes and Calaveras rivers were. For the second-largest storm, January 1997, both Cosumnes and San Joaquin rivers experienced extreme events, and Calaveras River did not. The third-largest storm occurred only on Sacramento River. Finally, for the fourth largest storm, March 1983, an extreme event occurred only on San Joaquin River. The risk assessment needs to be able to account for all of these possible inflow patterns.

The frequency analyses of Delta inflows described above resulted in 17 ranges of TDI and the probability that the annual peak daily inflow will be within a particular range. Estimates are provided for 5 different confidence limits ranging from 5 percent confidence that the inflow will not be exceeded to 95 percent confidence that the inflow will not be exceeded. The estimated probability of an inflow being in each of the 17 ranges is given in Table 7-7 for each of the 5 confidence limits. Note that the inflow probabilities in Table 7-7 represent a range of inflows equal to the referenced inflow plus and minus 1/34th of the difference in the natural logarithms of the total range of inflows considered in the studies.

The 17 bins resulting from the above analysis represent the range of inflows that are likely to occur in the Delta (i.e., from 0 to 3,000,000 cfs). The Risk Analysis will use the flow from each bin in the risk analysis to cover the range of possible inflows. For each flow is associated an annual probability that that flow will occur (the probabilities are included in Table 7-7). Because uncertainty exists in the estimate of the annual probability that a given flow will occur, the risk analysis will also associate a confidence bound with each annual probability, resulting in five estimates of the probability of occurrence for each inflow.

7.3 DELTA INFLOW PATTERNS

Inflow to the Delta is from several sources including the Yolo Bypass (Yolo), Sacramento River (Sac), Cosumnes River (CSMR), Mokelumne River (Moke), San Joaquin River (SJR), and miscellaneous streams (misc). Miscellaneous streams consist primarily of the Calaveras River. The sum of these sources of inflow is defined as the TDI. Given the variability of flows in the streams making up TDI, many combinations of flows that could account for any TDI observed are possible. This section describes a method for developing different combinations of Delta inflow patterns that could account for any selected TDI.

A somewhat arbitrary cutoff value of 200,000 cfs was selected to eliminate nonstorm event flow rates. A TDI of 200,000 cfs corresponds to a 50 percent confidence peak annual return period flow of about 3 years.

Flows in Sacramento River are not highly variable (the coefficient of variation is only 0.084) and that most of the variability is due to flows in Yolo Bypass. Flows in these two channels are not independent because the flows originate from the same watershed. Upstream of the City of Sacramento, when the stage in Sacramento River reaches the crest of Fremont Weir, flow in Sacramento River spills over the weir into Yolo Bypass. This spill condition occurs at a flow of about 55,000 cfs in Sacramento River, as measured below the weir. Most of the increase in flow above 55,000 cfs goes over the weir into Yolo Bypass. The Yolo Bypass Working Group et al. (2001) developed a relationship between flows in the Sacramento River below Fremont Weir and

spills over the weir. The relationship indicates that it is only necessary to be able to predict one of the stream flows (Sacramento River or Yolo Bypass), and the other stream flow can be estimated. For this reason, the method presented below is used to predict the sum of flow in Sacramento River and Yolo Bypass.

The methodology for estimating flow in any of the contributing tributaries to the Delta given a specified TDI is to use regression relationships for each contributing inflow. A constraint on the choice of the relationship is that for any TDI (even TDIs beyond what have been observed) the sum of the flows developed from the relationships must add up to the TDI. Therefore, the relationships cannot be independent of each other. The dependence between relationships was maintained by only applying the relationship to that portion of the flow not yet explained by any previously used relationship.

Table 7-8 lists the results of the logistic regression. The low r^2 values result from the large variability in the data. However, even with these small correlations, the equations reproduce the mean values for the flow distributions.

Figure 7-8 shows the results for the Sacramento River plus Yolo Bypass Delta inflow. The correlation coefficient for the fit is 0.94.

In addition to the above results, a relationship between the flow in Sacramento River and Yolo Bypass is needed to separate these two flows from the total. The correlation coefficient for the fit is 0.65. Figure 7-9 shows the relationship.

Figure 7-10 presents the results for San Joaquin River. The regression equations provide a reasonable fit, though it slightly underpredicts the main body of the data due to the small number of cases where the remaining flow is large and the fraction of flow in San Joaquin River is small (~10 percent of values). These events represent cases where a storm occurred on the Cosumnes River, but not the San Joaquin River.

Figure 7-11 presents the results for the miscellaneous inflows. The fit has an r^2 value of 0.94.

Figure 7-12 shows the results for the Cosumnes River. The r^2 value for the fit is 0.96, though it underestimates the peak annual flows.

The regression relationships reproduce the mean and median of the data well except for the median of Cosumnes River inflows. For most of the rivers, the mean flow is centered within the bulk of the observed flows (e.g., halfway between the 25th and 75th percentiles), whereas for Cosumnes River the mean is almost at the 75th percentile. This percentile implies that the distribution of inflows from Cosumnes River is more skewed than the inflows from other rivers and, therefore, the regression will not reproduce the median values as well. Figures 7-13 through 7-16 compare measured to predicted flow for the Sacramento River plus Yolo Bypass, San Joaquin River, miscellaneous inflows, and Cosumnes River, respectively. All of the figures show a very good fit between the measured and predicted flows except for the San Joaquin River cases in which the flows in other streams exceeded the flow in San Joaquin River. These values do not fit the relationship and need to be captured as part of the uncertainty analysis.

7.4 DELTA WATER SURFACE ELEVATIONS

Water surface elevations throughout the Delta that are associated with various flood magnitudes and inflow patterns are needed to estimate risks of levee failure due to overtopping and/or high

water. Water surface elevations in the Delta were estimated from data on historic water levels measured at selected Delta gauging stations. Water levels, or stages, at the selected gauging stations were then used to interpolate stages at intermediate locations in the Delta.

7.4.1 Data

Tide data used in these analyses are tide elevations measured at the Golden Gate Bridge (NOAA 2005). The Golden Gate Bridge tide station was chosen for its long record of unbroken tide data dating back about 150 years. Tide levels at the Golden Gate station are independent of inflows into the Delta while providing a geographically relevant measure of tailwater conditions that influence water levels in the Delta.

The California Data Exchange Center (CDEC) provides information on an extensive hydrologic data collection network, including automatic river stage sensors in the Delta. River stage data are provided primarily from the stations maintained by the DWR and USGS. The stage data can be downloaded from the CDEC's website (no date).

Stage data are provided on an hourly basis since 1984. For some gauging stations, 15-minute stage levels have been recorded for some inflow events since 1995. Figure 7-17 shows the locations of the stage gauging stations selected for use in these studies and presents the period of record for hourly and event data for each station. Gauging stations were selected based on station location and length and reliability of available record.

7.4.2 Data Review and Adjustments

Stage records for the selected gauging stations contained some inconsistent data that are significant enough to have an impact on the results of the analyses. To assist in evaluation of the stage data, plots of daily stage versus time were created for each of the measuring stations. These plots provide a picture of the normal stage range and also show apparent inconsistencies in the data. The data records were evaluated and, when possible, adjusted to eliminate apparent invalid data. The data records were reviewed to adjust or eliminate the following inconsistent data:

- Changes in Station Datum
- Measured Stages Greater Than Flood Stage
- Missing and Known Invalid Data
- Constant Stage Measurements
- Invalid Recording Intervals
- Incomplete Daily Records
- Conversion of Data to Common Datum

7.4.3 Regression Analysis of Water Surface Elevations

Once maximum daily stage data were reviewed, invalid records removed, and conversion to North American Vertical Datum 88 datum estimated for each station, the daily stage data for flood inflows were matched to the corresponding maximum daily tide data and the mean daily inflow data. The resulting data set is a daily record of maximum daily stage (North American

Vertical Datum 88 datum), maximum daily tide, and mean daily inflow from each of the six tributary inflows into the Delta.

This study focuses on the threat from high stages that occur during flood events. Most of the inflow data in the data sets represent low-inflow nonflood events. To minimize bias in the statistical analyses of water surface elevations, the inflow data sets were reduced to only include high inflow events. Based on review of the data it was judged that only TDI magnitudes greater than 57,000 cfs should be included in the regression analyses.

Using the data on maximum daily tide, mean daily inflow, and measured adjusted stages at the gauging stations, multiple regression analyses were made for each of the stage measuring stations. The regression analyses were made to determine best fit coefficients. To check that the local datums had been adjusted globally and to verify the equations, the calculated average stage elevations for historical total storm flows over 200,000 cfs were determined for each station and compared along the main Delta channels. Intermediate stage elevations between the selected gauging stations can be interpolated along the channel given the distance between the intermediate point and any two gauging stations and the predicted stage at the two gauging stations.

A map of water surface elevations for a 100-year event was developed for this project (DRMS 100-year map). These results were compared with 100-year flood results available in the literature, such as Federal Emergency Management Agency's (FEMA's) 100-year flood results. Figure 7-18 shows the comparison between DRMS and FEMA's 100-year flood levels for the Delta and Suisun Marsh area.

7.5 LEVEE FLOOD VULNERABILITY

This section addresses methods used to assess the vulnerability of levees and their foundations due to flood-induced risks.

7.5.1 Historic Failures

Since 1900, 166 islands have been flooded as a result of levee breaches in the Delta and Suisun Marsh. However, records on Suisun Marsh levee failures are incomplete. Table 7-9 summarizes the number of island/tract breaches and their corresponding years. Figure 7-19 illustrates the number of times islands or tracts breached since 1900. Figure 7-20 identifies the locations (when available) of the levee breaches that resulted in island/tract flooding. Most breach locations have been mapped except in the case of a few flood events for which the breach locations were not available.

A plot of island cumulative breach trend is presented on Figure 7-21. This plot should be viewed in the context of the historic changes the levee system has undergone in the last century. In recent years the levees have been built up to contain larger floods and have been upgraded/maintained to meet some engineering standards (freeboard, and attend to maintain stability). Part of the recent changes include (a) raising levees to meet higher flood protection level, (b) raising levees to compensate for foundation consolidation and settlement, (c) raising levees to mitigate for the continued subsidence (peat and organic marsh deposits) as a result of farming practices, and (d) improving/increasing maintenance to mitigate/contain the higher stresses on the levee system due to higher hydrostatic heads. Figure 7-21 should be considered an

overview of the historic evolution of the levee system performance. During the period since 1900, the average annual frequency of island flooding corresponds to about **1.57** expected flooded islands per year including all events exclusive of earthquakes (since earthquakes have not resulted in levee failures or damage). The trend of levee failure seems to indicate a slight improvement (1.32 average annual island flooding) for the period from 1951 to 2006 compared to 1.86 average annual island flooding for the period from 1900 to 1950. It is interesting to note that if the 11 flooded islands in 1950 are included in the last period (1950–2006), the trends for the two historic periods, 1900–1949 and 1950–2006, will be similar with 1.54 and 1.59 annual failure frequencies, respectively.

Figure 7-22(a) shows the cumulative number of levee breaches resulting in island flooding since 1950. The “sunny weather” island flooding events are excluded from these data. The data cutoff at 1950 was intentionally selected to remove the older historic events during which the levee configurations were dissimilar to the current levee conditions. These recent years represent a better data set to use for comparison with the results of the predictive levee analysis numerical models. One should recognize that since 1950, the levee geometry and crest elevation kept changing through time.

A further examination of the failure trends (Figure 7-22(a)) indicates an average annual frequency of flooded islands of **1.62** for the period between 1981 and 2006 compared to **0.87** for the period between 1951 and 1980. These trends indicate that during the recent 26 years, the Delta and Suisun Marsh have experienced a higher number of flooded islands and tracts than the period between 1951 and 1980 (30 years) despite the increasing maintenance efforts and subvention programs. Figure 7-22(b) shows the Delta levees program funding since 1982. To better understand the higher occurrence of island flooding events in the last 26 years, a flow hydrograph (since 1955, available records) is presented on Figure 7-22(c). The total in-flow hydrograph shows that the storm events recorded since 1980 are more potent and characterized by higher magnitudes than the storms recorded in the 25 years prior to 1980. Furthermore, the higher magnitude storm events, since 1980, correlate with higher number of flooded islands/tracts. These particular events include the 1980 (5 islands flooded), 1983 (11 islands flooded), 1986 (9 islands flooded), and 1997 (11 islands flooded). The higher frequency of island flooding in the last 26 years seems to have a strong correlation with the larger storms events compared to the 1951–1980 period of storm records.

7.5.2 Flood Failure Modes

Three main modes of failures, through-seepage, underseepage, and overtopping, were considered to estimate the risk associated with flooding for this project. The erosion and slope instability were not considered as one of the main modes of failures but they were considered as fraction of total mode of failures. For example, the through-seepage emanating from landside slope of the levee could lead to slope instability.

Current practice is to separate levee seepage into two general categories: underseepage and through-seepage. Underseepage refers to water flowing under the levee in the underlying foundation materials, often emanating from the bottom of the landside slope and ground surface extending landward from the landside toe of the levee. Through-seepage refers to water flowing through the levee prism directly, often emanating from the landside slope of the levee. Both conditions can lead to failures by several mechanisms, including excessive water pressures

causing foundation heave and slope instabilities, and immediate and progressive internal erosion, often referred to as piping.

Under- and through-seepage are both manifestations of essentially the same mechanism; seepage-induced water pressures are high enough to internally erode materials and/or cause soil instabilities. Each can progress to complete failure of the levee. Combined with knowledge about the levee and foundation materials and their variability, both under- and through-seepage can be evaluated qualitatively and/or quantitatively using standard principles of soils and hydraulic engineering.

Our review of past failures included review of reports and interviewing local and state employees. For most of the past failures, information regarding mode of failure, time and date of failure, and water level in the slough are either not available at all or very limited. Therefore, the allocation of number of failures to different mode of failure was based on engineering judgment and experience of Vulnerability team members. No supporting documents are available to verify our assumption regarding the mode of failure. The Vulnerability team believes 80 percent of the past failures can be attributed to seepage-induced failures. The team also believes that both through- and underseepage-induced failures occurred in equal numbers. The remaining 20 percent of past failures can be attributed to overtopping.

7.5.2.1 Underseepage

Excessive underseepage is often accompanied by the formation of sand boils. Boils often look like miniature volcanoes, ejecting water and sediments, usually due to high underseepage pressures. These boils can lead to progressive internal erosion, undermining, and levee failure. Boils have been widely observed in all of the historic floods and are believed to have caused significant failures in 1986 and 1997.

7.5.2.2 Through-Seepage

Excessive through-seepage often leads to levee landside slope stability problems. At almost all locations, Delta levees are comprised of either dredged, clean, highly permeable river sands, or interbedded layers of organic and mineral soils with contrasting permeabilities. During high water conditions, because of their high permeability and layering, these materials will allow large volumes of water to flow through the levee, at rates high enough to cause internal erosion and slope instability. Often, water is seen exiting the landside slope of the levee, above the landside toe. As this increases, slumping of the levee slopes is often seen progressing from surficial slumps to complete rotation and/or translation of the levee prism and eventual breach of the levee.

The majorities of the Delta and Suisun Marsh levees have some pervious materials within the embankments and can therefore transmit water. It is believed that developing a failure model for predicting through-seepage induced failures considering the record of past failures is much more reliable than performing a series of seepage model analyses. The accuracy and usefulness of the failure model can be improved by checking it against a record of actual recorded events and adjusting it if necessary.

7.5.2.3 Overtopping

The overtopping failure occurs when the floodwater level rises above the crest of a levee. The main factors required for assessment of the probability of overtopping are levee crest elevation and the probability of floodwater levels exceeding this elevation. Note that, in some locations some amount of overflow can occur without complete failure of the levee. The human intervention can also result in preventing the overtopping failure by raising the crests with sandbags during high water periods. Computations of the probability of failure in overtopping were conducted by evaluating the probability of a given flood and the corresponding water level in excess of the measured crown elevations of levees. The probability of failure in overtopping was estimated using the fragility curve, which was developed using experts' elicitation (Figure 7-23). The flood levels for current and future years (50, 100, and 200 years from now) were developed by the Flood Hazard Team. The probability of overtopping during current and future years was assessed using the fragility curve for overtopping, levee crest elevations, and flood frequency and stage values provided by the Flood Hazard Team.

7.5.2.4 Erosion

The mode of failure associated with streamflow erosion and wind-wave induced erosion is addressed in Chapters 8 and 10.

7.5.3 Flood Vulnerability Approach

Underseepage analyses were conducted using steady-state analysis procedures of the finite element program Seep/W (Geo-Slope International Ltd. 2004). Models in this program were developed using two-dimensional, planar and isoparametric and higher-order finite elements models. The program can model multiple soil types, each having different anisotropic hydraulic conductivity characteristics to model the behavior of essentially all soil-types encountered in the Delta.

Boundary conditions in the steady-state analyses were modeled as a variety of conditions, including constant head, no-flow, constant flow or variable, based on in-situ conditions expected for each model. Infinite elements can also be included in the model section to model and infinite half-space at the edge of the model.

Water levels in the low-lying Delta islands are maintained 2 to 5 feet below land surface by an extensive network of drainage ditches, and accumulated agricultural drainage is pumped through or over the levees into stream channels. Therefore, it is reasonable to assume that steady-state seepage conditions exist in the tidal Delta and Suisun Marsh for the purpose of calibrating models and developing fragility curves. In the northern Delta and in the Delta fringes, floodwaters may rise and then drop fast enough that full steady state conditions may not always develop in every area, especially if the foundation materials are of low permeability. In these locations, steady-state analyses may slightly overestimate seepage conditions, but because of the low permeability, these areas will likely not be vulnerable to significant underseepage problems. Conversely, based on observations from past floods, most, if not all of the levees that have underseepage problems are founded on materials that are relatively permeable, where steady-state seepage analyses are appropriate.

7.5.4 Vulnerability Classes

The system of levees in the Delta study area was divided into vulnerability classes using factors that differentiate the performance of the levees when subjected to the same flood event. The factors considered in defining levee vulnerability classes were:

- Thickness of peat and organics (0, 0.1-5 ft, 5.1-10 ft, 10.1-15 ft, 15.1-30 ft, and >30 ft)
- Slough width (narrow (<500 ft), not narrow (>500 ft))
- Presence of slough sediment (presence, not presence) and
- Presence of toe drainage ditch (presence, not presence)

The main variables in defining under-seepage vulnerability classes were thickness of peat and organics, and slough width. The vulnerability classes for Delta and Suisun Marsh were developed considering all possible combinations of these main variables. The variations in the permeability of peat, the variations in peat and organic layer thickness, presence of slough sediment, and presence of drainage ditch were treated as random input variables, where applicable (see Table 7-10). For example, vulnerability class 1 has presence of slough sediment and presence of drainage ditch as random input variables; other potential random variables are not applicable because the vulnerability class has no effect of peat. Conversely, vulnerability class 3 has presence of slough sediment, presence of drainage ditch, thickness of peat and organics, and permeability of peat as random input variables. Table 7-10 lists the vulnerability classes considered for under-seepage analyses for Delta and Suisun Marsh area along with the random input variables for each vulnerability class. The probability distribution of variations in peat and organic layer thickness within a vulnerability class was defined based on a statistical analysis of available data. Randomness in presence of slough sediment and presence of toe drainage ditch were individually assumed to have 50% chance of occurrence.

7.5.5 Results of Underseepage Analyses

To develop fragility curves representative of conditions throughout the Delta, seepage models with the range of subsurface conditions throughout the Delta were developed and analyzed. As shown on the peat/organic soil thickness map (Figure 6-34), the thickness of a landside blanket layer varies throughout the Delta. Therefore, a series of models with a layer of lower permeability blanket materials varying in thickness from 5 to 35 feet were developed. For each of these models, “with ditch” and “without ditch” models were considered.

Several other factors were considered in these models. Based on anecdotal evidence, field experience, and limited available slough boring data, it was decided that blanket layer, often comprised of peat/organic soils would be terminated below the waterside toe of the slope. Based on a review of available data and from past modeling experience, the bottom elevation of foundation sands was set at -80 feet. To model the landside downward slope of the ground surface away from most Delta levees, a slope of about 500H:1V was used. If the section was modeled with drainage ditch, the ditch was modeled as being 5 feet deep and located approximately 100 feet away from levee centerline. Based on a review of the available bathymetry data, the average slough dimensions were modeled as having an average width of 600 feet and average bottom elevation of -25 feet. For the cases modeling the presence of slough

bottom sediments, a 2-foot-thick lower permeability fine-grained soil was included in the models.

Figures 7-24 (a) to (d) present the computed vertical gradients for a 15-foot-thick blanket layer as a function of river/slough water levels for “with” and “without” ditch, respectively. Review of these results indicates that the vertical gradient under the ditch increase to values ranging from 0.8 to 1.6 as a function of higher water levels (Figure 7-24(a)) effectively representing the average gradient through a 10-foot-thick blanket. On the other hand, the vertical gradients calculated for the case without the ditch are smaller and range from 0.4 to 0.9 near the toe (Figure 7-24(c)) and 0.3 to 0.8 away the toe (Figure 7-24(d)).

Multiple regression equations were developed (mean value and distribution around the mean) to represent the seepage gradient as a function of crest elevation minus water surface elevation for various confidence levels (called levee “response” curves).

Members of the Levee Vulnerability Team and the DRMS Technical Advisory Committee were given summary presentations regarding the above data compilations, model development, model results, and final developed relationships between computed gradients as a function of water levels and blanket permeability. In addition, this group of experts was asked to make the following assumptions:

1. The intention behind the development of this relationship is to characterize the likelihood that erosion and piping will progress to the point of full “failure” (breaching).
2. High water persists for one to several days (or so) with tides causing some fluctuation, but the principal source of high water risk is high flood levels.
3. In some cases, but not all cases, pre-existing partial erosion degradation may already be present from previous events.

With the model results and above assumptions as a uniform basis for evaluation, this group of experts was then asked to independently develop estimates of the probability of failure as a function of vertical gradient. Each separately submitted a spreadsheet showing their estimated probability of failure as a function of vertical gradient. They were then asked to estimate the probability of failure for the same situation, but with human intervention initiated at an appropriate level at that location. These curves were compiled and statistically analyzed.

Figure 7-25 presents a summary of the results of this exercise, assuming no human intervention. As shown, the mean value of the probability of failure is less than 50 percent for computed vertical gradients of less than 0.8. Probabilities of failure are expected to be greater than 80 percent when the vertical gradient is greater than about 1.1. This value is in general agreement with values suggested by the US Army Corps of Engineers (USACE 1999).

Figure 7-26 presents a summary of the results of this exercise, assuming human intervention. Comparison of Figure 7-25 with Figure 7-26 indicates that the expert panel believes that human intervention, unimpeded by resource constraints, can significantly reduce the probability of failure for a levee, as indicated by the significant shift of the mean value curves to the right on the graphs.

The seepage gradient versus crest elevation minus water surface elevation curves are combined with the probability of failure versus gradient curves to produce the probability of failure versus crest elevation minus water surface elevation (flood stage) for the entire Delta and Suisun Marsh

for each vulnerability class, as illustrated on Figure 7-27. The Levee Vulnerability Team believes these curves represent a reasonable numerical model to assess flood induced underseepage fragility of levees in both the Delta and Suisun Marsh. The resulting curves represented by Figure 7-27 (also presented in Table 7-11) are the basic input to the risk model.

7.6 FLOOD SYSTEMS MODEL

7.6.1 Spatial Modeling of Physical Response of Levees to Flood Events

Section 7.5 described the geotechnical model used to assess seepage gradients of individual levees in different vulnerability classes subjected to a given flood scenario and the probability model to assess the probability of a breach of a levee reach given the estimated seepage gradient. To assess the risk of simultaneous, multiple levee failures under a given flood, the simultaneous physical behavior of all levees in the study area subjected to a specified flood event also needs modeling. Such a model needs to account for the spatial continuity of levees and define how levees within and across levee reaches are likely to behave in a given flood event.

This section first provides an overview of the spatial physical model of representing levees around different islands and describes the key assumptions made in modeling the spatial behavior of levees during a flood event.

The geotechnical fragility model described in Section 7.6.1 provides a procedure to estimate the probability of underseepage failure on individual reaches of an island. This procedure needs to be extended for estimating the probability of underseepage failure of an island. The approach is based on the concept of the “weakest” link; that is, the first failure of a system would occur at the weakest link. This assumption is appropriate for a linear system such as levees. It would not be known with certainty which levee reach is the weakest link. It is reasonable to assume that each reach has some probability of being the weakest link and that probability is proportional to the vulnerability of the reach as reflected in its conditional failure probability. That is, a reach with a higher failure probability would be more vulnerable to a failure, and would have a greater chance of being the weakest link and failing first. Using this assumption, the probability that each reach on an island is the weakest link is first estimated by making this probability proportional to the reach failure probability. This estimation can then be used to calculate the joint probability that a given reach would be the weakest link and would fail. This joint probability is summed over all reaches to estimate the probability of failure of the island.

This approach will honor three essential criteria. One, it will be invariant with regard to the reach length. That is, one would get the same answer whether an island is divided into 10 reaches or 100 reaches. Second, it will preserve the concept of the weakest link. That is, the probability of island failure would not be simply an average value over all reaches. Third, each reach will contribute to the overall probability of island failure. That is, the probability of island failure will not be controlled by a single reach that has the maximum failure probability. This approach simply reflects the fact that it is not known with certainty which reach is the weakest link; each reach could be the weakest link, with some probability, and could fail first.

Let,

f_{ijk} = conditional underseepage failure probability of j-th reach on i-th island for k- th flood event

$f_{i,k}$ = conditional underseepage failure probability of i-th island for k-th flood event

w_{ijk} = probability that j-th reach on i-th island is the “weakest” link for k-th event (that is, the link that would fail first under the given event)

w_{ijk} is calculated as follows:

$$w_{ijk} = f_{ijk} / \sum(f_{ijk}) \quad (1)$$

The conditional underseepage failure probability of the i-th island for k-th event is calculated taking into account the probability that each reach could be the weakest link and the conditional underseepage failure probability of that reach for k-th event. Thus, $f_{i,k}$ is calculated from:

$$f_{i,k} = \sum_j (w_{ijk} f_{ijk}) \quad (2)$$

7.6.2 Island Failure Probability Under Multiple Failure Modes

The previous section was used to estimate the probability of an island failure in underseepage for a given flood event. The probability of an island failure in through-seepage was assumed to be equal to the probability of failure in underseepage as discussed in Section 7.5.1. The probability of an island failure in overtopping was estimated using the procedure described in Section 7.5.1 (i.e., using the fragility curve for overtopping). Overall probability of an island failure due to any of these three failure modes was calculated as follows:

$$P_f(\text{island}) = 1 - ((1 - P_{fUS}) \times (1 - P_{fTS}) \times (1 - P_{fOT})) \quad (3)$$

Where,

$P_f(\text{island})$ = Probability of an island failure

P_{fUS} = Probability of an island failure in underseepage

P_{fTS} = Probability of an island failure in through-seepage

P_{fOT} = Probability of an island failure in overtopping

7.6.3 Probability of Damaged Levees

A damaged levee section due to underseepage during a flood event is likely to show such signs as sand boils and scour holes. Experience with inspection and repairs of such damaged levees suggests that the average contiguous levee length with intermittent signs of damage is of the order of 5,000 feet. Furthermore, for each breach, 5 to 10 miles of levees, on the average, show signs of damage. Assuming a midpoint of 8 miles for the average miles of damaged levees for each breach, a typical length 5,000 feet of each contiguous damaged levee, and a typical length of 20,000 feet for a contiguous spatial zone, one would get, on the average, about 4 levee sections with damage potential per contiguous spatial zone. The average number of levee sections that are damaged would be about 8 per breach. If the breach rate is say m/n , the damaged levee rate would be $8m/4n = 2(m/n)$. Thus, the probability of damaged levee section would be about twice that of a breach in a given contiguous spatial zone.

7.6.4 Length Effects on Probability Assessment

The procedure presented above for the estimation of an island failure probability does not account for the effect of length of levees within each island. A simplified procedure was developed using empirical observations to adjust the probability of failure considering the length of each island under consideration. To develop this simplified procedure, first islands that have breached multiple times in the past were looked for (e.g., Venice Island breached 8 times in the past 100 years). This island can be considered as the reference case where all contributing effects (including length) are included. Hence, the length effect is developed as simple hyperbolic scaling function as described in Equation (4). This factor (SF) is used to adjust the probability of failure of any given island.

$$\text{Scaling Factor (SF)} = 1 + (L_i - L_r) / L_n \quad (4)$$

Where,

L_i = length of an island under consideration

L_r = length of a referenced island

L_n = length of the longest island in the study area

Tables

Table 7-1 Partial List of Major Dams and Reservoirs in Tributary Watersheds to the San Francisco Bay-Delta

Dam Name	Watercourse	Tributary of	Reservoir	Year Original Construction Completed	Reservoir Capacity (acre-feet)
East Park	Little Stony Creek	Sacramento River	East Park	1910	
Daguerre Point	Yuba River	Sacramento River		1910	
Cache Creek	Cache Creek	Sacramento River	Clear Lake	1914	
Capay Diversion Dam	Cache Creek	Sacramento River		1914	
Stony Gorge	Stony Creek	Sacramento River	Stony Gorge	1928	
Pardee	Mokelumne River	San Joaquin River	Pardee	1929	210,000
Englebright	Yuba River	Sacramento River		1941	
Friant	San Joaquin River	San Joaquin River	Millerton Lake	1942	520,000
Shasta	Sacramento River	Sacramento River	Shasta Lake	1945	4,552,000
Martinez	off-stream storage		Martinez	1947	
Keswick	Sacramento River	Sacramento River	Keswick	1950	
Sly Park	Sly Park Creek	American / Sacramento River	Jenkinson Lake	1955	
Mormon Island Auxiliary Dam	Blue Ravine	American / Sacramento River	Folsom Lake	1956	
Folsom	American River	Sacramento River	Folsom Lake	1956	1,010,000
Tulloch	Stanislaus River	San Joaquin River	Tulloch	1957	68,000
Monticello	Putah Creek	Sacramento River	Lake Berryessa	1957	
Comanche	Mokelumne River	San Joaquin River	Comanche	1963	431,000
Whiskeytown	Clear Creek	Sacramento River	Whiskeytown Lake	1963	
Spring Creek Debris Dam	Spring Creek	Sacramento River	Spring Creek	1963	
Red Bluff (Diversion)	Sacramento River	Sacramento River	Lake Red Bluff	1964	
New Hogan	Calaveras River	San Joaquin River	New Hogan	1931, 1964	325,000
Los Banos (Detention)	Los Banos Creek	San Joaquin River	Los Banos	1965	

Table 7-1 Partial List of Major Dams and Reservoirs in Tributary Watersheds to the San Francisco Bay-Delta

Dam Name	Watercourse	Tributary of	Reservoir	Year Original Construction Completed	Reservoir Capacity (acre-feet)
Little Panoche (Detention)	Little Panoche Creek	San Joaquin River	Little Panoche	1966	
San Luis	San Luis Creek	Delta - Mendota Canal	San Luis	1967	
O'Neill	San Luis Creek	Delta - Mendota Canal	O'Neill Forebay	1967	
Contra Loma	off-stream storage		Contra Loma	1967	
Oroville	Feather River	Sacramento River	Lake Oroville	1968	3,537,580
New Exchequer	Merced River	San Joaquin River	Lake McClure	1926, 1968	1,026,000
New Bullards Bar	Yuba River	Sacramento River	New Bullards Bar	1969	
New Don Pedro	Tuolumne River	San Joaquin River	New Don Pedro	1923, 1971	2,030,000
Buchanan	Chowchilla River	San Joaquin River	Eastman Lake	1975	150,000
Indian Valley	N Fork Cache Creek	Sacramento River	Indian Valley	1976	300,600
New Melones	Stanislaus River	San Joaquin River	New Melones	1979	2,400,000
Sugar Pine	N Shirttail Creek	American / Sacramento River	Sugar Pine	1981	
Hidden	Fresno River	San Joaquin River	Hensley Lake		90,000
Almanor	N Fork Feather River	Sacramento River			

Table 7-2 Summary of Delta Inflows

Sacramento + Yolo Bypass Inflows	WY 1956 - 1968, pre-Oroville Dam	WY 1969 - 2005, ~Existing Conditions	WY 1956 - 2005, Period of Record
Average Daily Inflow, cfs	26,430	28,671	28,088
Avg. Annual Precip., inches¹	17.4	18.1	18
Max. Annual Precip., inches	27.7	34.5	35
Inflow Range	Number of Inflows in Q-Range		
0-100K	4564	12924	17488
100K-200K	152	466	618
200K-300K	28	96	124
300K-400K	3	19	22
400K-500K	2	5	7
>500K	0	4	4
sum =	4749	13514	18263
Inflow Range	No. of Days per Year With Inflows in Q-range		
0-100K	351.1	349.3	349.8
100K-200K	11.7	12.6	12.4
200K-300K	2.2	2.6	2.5
300K-400K	0.2	0.5	0.4
400K-500K	0.2	0.1	0.1
>500K	0.0	0.1	0.1
sum =	365.3	365.2	365.3

San Joaquin River Inflows	WY 1956 - 1979, pre-New Melones Dam	WY 1980 - 2005, ~Existing Conditions	WY 1956 - 2005, Period of Record
Average Daily Inflow, cfs	4,416	4,809	4,416
Avg. Annual Precip., inches²	13.9	14.9	14.3
Max. Annual Precip., inches	25.9	27.5	27.5
Inflow Range	Number of Inflows in Q-range		
0-10K	8037	8270	16307
10K-20K	393	697	1090
20K-30K	247	336	583
30K-40K	74	171	245
40K-50K	15	22	37
>50K	0	1	1
sum =	8766	9497	18263
Inflow Range	No. of Days per Year With Inflows in Q-range		
0-10K	334.9	318.1	326.1
10K-20K	16.4	26.8	21.8
20K-30K	10.3	12.9	11.7
30K-40K	3.1	6.6	4.9
40K-50K	0.6	0.8	0.7
>50K	0.0	0.0	0.0
sum =	365.3	365.3	365.3

¹ Precipitation data from the Sacramento Airport, Station 47630.

² Friant Government Camp.

SECTION SEVEN

Flood Risk Analysis

Table 7-3 Annual Peak Day Delta Inflows of Record (Water Years 1956 Through 2005)

Water Year	Date, WY Peak Inflow Day	Peak Day Sacramento River, cfs	Peak Day Yolo Bypass, cfs	Peak Day Cosumnes River, cfs	Peak Day Mokelumne River, cfs	Peak Day Misc. Streams, cfs	Peak Day San Joaquin River, cfs	Peak Day Total Inflow, cfs	Average 5-day Peak Inflow, cfs	Ratio: Avg. 5-day Peak to Peak Day	5-Day Inflow Vol. Up Through Peak Day, ac-ft
1986	February 20, 1986	113,000	499,301	15,600	4,490	14,981	13,900	661,272	551,714	0.83	4,501,390
1997	January 3, 1997	113,000	395,140	19,200	4,250	5,699	24,700	561,989	493,338	0.88	3,641,897
1965	December 25, 1964	98,600	343,265	11,500	150	2,607	14,000	470,122	382,948	0.81	2,673,209
1983	March 4, 1983	83,100	274,300	6,490	3,350	13,173	41,800	422,213	381,167	0.90	3,127,847
1995	March 13, 1995	96,100	266,562	6,340	2,440	1,635	14,100	387,177	336,016	0.87	2,229,884
1970	January 25, 1970	93,000	255,600	5,970	4,330	3,821	21,200	383,921	362,105	0.94	3,304,076
1956	December 23, 1955	90,200	249,600	34,100	2,180	4,032	3,210	383,322	276,247	0.72	1,571,520
1984	December 28, 1983	92,700	221,988	7,010	3,840	7,484	18,600	351,622	305,986	0.87	2,345,681
1963	February 2, 1963	94,400	230,107	17,300	3,260	1,962	3,830	350,859	202,799	0.58	1,190,319
1980	February 22, 1980	94,100	202,145	9,190	1,730	11,543	20,300	339,008	303,426	0.90	2,285,050
1998	February 8, 1998	86,800	193,521	6,130	2,930	7,331	26,300	323,012	305,585	0.95	2,823,322
1969	January 27, 1969	87,000	134,770	10,600	4,160	5,480	41,700	283,710	259,060	0.91	2,608,721
1958	February 26, 1958	85,500	174,510	6,140	1,650	3,276	7,750	278,826	245,784	0.88	2,281,874
1974	January 20, 1974	94,200	165,350	4,360	2,250	1,642	8,290	276,092	251,157	0.91	1,960,832
1982	February 17, 1982	98,000	103,742	11,700	3,030	14,203	7,720	238,395	175,241	0.74	1,041,400
1967	February 1, 1967	90,100	132,590	6,060	93	918	8,070	237,831	211,254	0.89	1,807,500
1973	January 19, 1973	92,700	112,559	6,790	1,910	2,472	6,370	222,801	196,152	0.88	1,728,843
1996	February 23, 1996	86,800	93,818	2,900	2,840	5,262	15,400	207,020	193,127	0.93	1,647,205
2004	February 28, 2004	73,800	105,288	1,500	326	1,050	4,220	186,184	177,486	0.95	1,594,217

SECTION SEVEN

Flood Risk Analysis

Table 7-3 Annual Peak Day Delta Inflows of Record (Water Years 1956 Through 2005)

Water Year	Date, WY Peak Inflow Day	Peak Day Sacramento River, cfs	Peak Day Yolo Bypass, cfs	Peak Day Cosumnes River, cfs	Peak Day Mokelumne River, cfs	Peak Day Misc. Streams, cfs	Peak Day San Joaquin River, cfs	Peak Day Total Inflow, cfs	Average 5-day Peak Inflow, cfs	Ratio: Avg. 5-day Peak to Peak Day	5-Day Inflow Vol. Up Through Peak Day, ac-ft
1978	January 18, 1978	75,000	85,024	5,100	114	5,062	4,150	174,450	158,930	0.91	1,310,340
2000	February 28, 2000	81,700	63,375	5,010	2,010	3,071	13,600	168,766	156,851	0.93	1,446,424
1962	February 16, 1962	70,100	68,679	7,520	547	2,826	7,820	157,492	137,722	0.87	1,131,743
1993	March 28, 1993	82,300	53,026	3,280	431	662	3,950	143,649	136,829	0.95	1,300,621
1960	February 10, 1960	69,100	67,482	3,280	156	712	2,130	142,860	108,434	0.76	741,241
1999	February 11, 1999	85,400	31,150	3,630	2,770	6,568	11,900	141,418	124,608	0.88	991,787
1975	March 26, 1975	73,800	36,228	6,340	895	3,171	6,930	127,364	118,869	0.93	1,126,078
1957	March 7, 1957	79,200	36,361	4,050	1,800	1,024	4,690	127,125	112,424	0.88	959,768
1959	February 20, 1959	67,300	46,902	1,830	662	1,404	4,840	122,938	105,502	0.86	797,068
1971	December 5, 1970	73,200	32,983	5,880	1,230	1,675	3,640	118,608	108,748	0.92	923,631
2002	January 6, 2002	65,567	34,528	725	194	3,097	4,224	108,335	91,437	0.84	802,132
1979	February 24, 1979	71,300	5,170	2,660	1,260	7,856	12,800	101,046	95,445	0.94	838,080
2005	May 22, 2005	74,100	6,668	1,590	2,090	151	12,100	96,699	90,974	0.94	769,349
2003	January 3, 2003	65,300	25,560	261	211	154	2,280	93,766	83,057	0.89	751,934
1968	February 25, 1968	66,200	18,648	1,350	838	1,251	4,120	92,407	88,976	0.96	798,413
1989	March 27, 1989	73,500	26	1,820	7	11	2,020	77,384	68,450	0.88	578,604
1966	January 10, 1966	53,600	4,085	377	436	536	5,350	64,384	61,741	0.96	596,854
1981	January 31, 1981	51,900	5,096	759	72	741	5,700	64,268	60,686	0.94	525,396
1964	January 23, 1964	52,200	2,841	2,780	624	455	3,110	62,010	54,099	0.87	399,078

Table 7-3 Annual Peak Day Delta Inflows of Record (Water Years 1956 Through 2005)

Water Year	Date, WY Peak Inflow Day	Peak Day Sacramento River, cfs	Peak Day Yolo Bypass, cfs	Peak Day Cosumnes River, cfs	Peak Day Mokelumne River, cfs	Peak Day Misc. Streams, cfs	Peak Day San Joaquin River, cfs	Peak Day Total Inflow, cfs	Average 5-day Peak Inflow, cfs	Ratio: Avg. 5-day Peak to Peak Day	5-Day Inflow Vol. Up Through Peak Day, ac-ft
2001	March 9, 2001	46,200	4,425	483	289	627	5,660	57,684	53,441	0.93	505,557
1992	February 17, 1992	46,800	2,456	1,290	177	1,516	5,110	57,349	53,943	0.94	495,923
1991	March 27, 1991	46,900	3,260	1,310	119	2,027	3,310	56,926	49,859	0.88	398,339
1961	February 14, 1961	49,500	1,750	228	111	36	960	52,585	51,222	0.97	455,516
1985	November 30, 1984	41,200	3,408	511	762	439	3,500	49,820	47,470	0.95	461,516
1987	March 16, 1987	38,000	1,686	840	91	443	3,000	44,060	40,764	0.93	331,279
1988	January 7, 1988	37,200	3,245	203	46	49	1,280	42,023	39,287	0.93	291,814
1990	January 16, 1990	36,900	25	284	45	30	1,370	38,654	33,325	0.86	293,407
1972	December 28, 1971	31,100	192	1,440	96	406	3,430	36,664	35,424	0.97	337,839
1994	February 10, 1994	29,900	1,686	190	150	64	2,780	34,770	29,317	0.84	237,051
1976	December 8, 1975	30,600	48	53	297	15	3,580	34,593	33,457	0.97	325,369
1977	January 5, 1977	13,700	3	76	37	12	1,080	14,908	13,128	0.88	122,450

Table 7-4 Annual Peak Delta Inflows (cfs), 1956-2005

Water Year	Water Year Oct. 1 to Sept. 30	High Runoff Season Dec 16 to Apr 15	Low Runoff Season Oct 1 to Dec 15, Apr 16 to Sep 30
1956	383,322	383,322	80,086
1957	127,125	127,125	77,800
1958	278,826	278,826	127,867
1959	122,938	122,938	18,357
1960	142,860	142,860	21,479
1961	52,585	52,585	35,461
1962	157,492	157,492	35,160
1963	350,859	350,859	232,438
1964	62,010	62,010	42,188
1965	470,122	470,122	90,923
1966	64,384	64,384	38,415
1967	237,831	237,831	115,781
1968	92,407	92,407	25,433
1969	283,710	283,710	86,471
1970	383,921	383,921	26,488
1971	118,608	110,400	118,608
1972	36,664	36,664	22,654
1973	222,801	222,801	43,742
1974	276,092	276,092	123,106
1975	127,364	127,364	44,033
1976	34,593	30,651	34,593
1977	14,908	14,908	12,438
1978	174,450	174,450	70,752
1979	101,046	101,046	27,774
1980	339,008	339,008	33,394
1981	64,268	64,268	33,434
1982	238,395	238,395	197,768
1983	422,213	422,213	127,334
1984	351,622	351,622	169,189
1985	49,820	44,937	49,820
1986	661,272	661,272	48,018

Table 7-4 Annual Peak Delta Inflows (cfs), 1956-2005

Water Year	Water Year Oct. 1 to Sept. 30	High Runoff Season Dec 16 to Apr 15	Low Runoff Season Oct 1 to Dec 15, Apr 16 to Sep 30
1987	44,060	44,060	26,604
1988	42,023	42,023	28,941
1989	77,384	77,384	30,508
1990	38,654	38,654	23,052
1991	56,926	56,926	13,399
1992	57,349	57,349	13,870
1993	143,649	143,649	54,362
1994	34,770	34,770	29,893
1995	387,177	387,177	176,174
1996	207,020	207,020	98,021
1997	561,989	561,989	130,890
1998	323,012	323,012	112,420
1999	141,418	141,418	69,997
2000	168,766	168,766	43,293
2001	57,684	57,684	18,567
2002	108,335	108,335	39,772
2003	93,766	93,766	71,627
2004	186,184	186,184	34,270
2005	96,699	73,956	96,699

Table 7-5 Results of Log Pearson Type III Frequency Analyses

Probability	Inflows For Various Percent Confidence That The Inflow Will Not Be Exceeded												
	CL = 99%	CL = 97.5%	CL = 95%	CL = 90%	CL = 80%	CL = 60%	CL = 50%	CL = 40%	CL = 20%	CL = 10%	CL = 5%	CL = 2.5%	CL = 1%
All Seasons Inflow													
0.5000	183,628	174,123	167,003	159,301	150,600	139,862	135,551	131,292	121,982	115,391	110,149	105,728	100,438
0.2000	417,743	384,177	362,404	340,001	316,076	288,481	280,047	267,913	246,965	232,973	222,322	213,661	205,125
0.1000	646,984	583,006	543,290	503,306	461,634	414,947	402,011	381,158	347,674	325,861	309,564	296,514	284,711
0.0500	925,781	819,574	755,468	691,963	626,943	555,619	536,997	505,080	455,965	424,523	401,337	382,966	367,245
0.0400	1,026,698	904,163	830,738	758,322	684,543	604,074	583,366	547,383	492,578	457,658	431,996	411,722	394,606
0.0250	1,257,855	1,096,264	1,000,731	907,312	813,021	711,305	685,788	640,424	572,582	529,736	498,454	473,871	453,614
0.0200	1,376,716	1,194,262	1,087,010	982,520	877,483	764,716	736,715	686,503	611,966	565,071	530,929	504,158	482,312
0.0100	1,784,960	1,527,536	1,378,571	1,234,957	1,092,240	941,059	904,505	837,586	740,151	679,497	635,677	601,532	574,362
0.0050	2,255,260	1,906,317	1,707,080	1,516,767	1,329,544	1,133,535	1,087,120	1,000,928	877,353	801,129	746,428	704,032	670,944
0.0020	2,978,735	2,480,798	2,200,802	1,936,227	1,679,002	1,413,366	1,351,820	1,236,059	1,072,812	973,177	902,221	847,564	805,745
0.0010	3,607,958	2,974,111	2,621,311	2,290,391	1,971,236	1,644,691	1,570,048	1,428,709	1,231,467	1,111,939	1,027,254	962,289	913,176
0.0005	4,312,097	3,520,576	3,084,102	2,677,476	2,288,198	1,893,304	1,804,086	1,634,300	1,399,532	1,258,192	1,158,523	1,082,350	1,025,346
0.0001	6,257,320	5,006,780	4,330,189	3,708,698	3,122,771	2,538,809	2,409,770	2,162,386	1,826,400	1,626,823	1,487,440	1,381,729	1,304,080
High Inflow Season													
0.5000	181,568	172,677	165,544	157,831	149,124	138,385	134,031	129,820	120,522	113,944	108,714	104,307	99,311
0.2000	413,058	384,136	362,145	339,533	315,401	287,591	276,906	266,882	245,805	231,739	221,037	212,338	202,824
0.1000	639,727	585,479	545,194	504,669	462,468	415,235	397,502	381,085	347,276	325,268	308,836	295,684	281,518
0.0500	915,397	825,972	760,721	696,137	630,079	557,696	530,974	506,465	456,730	424,919	401,476	382,913	363,125
0.0400	1,015,182	912,153	837,341	763,625	688,596	606,861	576,822	549,344	493,801	458,443	432,477	411,975	390,180
0.0250	1,243,746	1,108,170	1,010,641	915,363	819,299	715,802	678,096	643,769	574,902	531,453	499,753	474,855	448,526
0.0200	1,361,275	1,208,309	1,098,719	992,060	884,962	770,130	728,451	690,588	614,872	567,283	532,662	505,531	476,903
0.0100	1,764,939	1,549,465	1,396,870	1,249,918	1,104,061	949,770	894,360	844,316	745,139	683,467	638,948	604,280	567,919
0.0050	2,229,964	1,938,146	1,733,590	1,538,429	1,346,685	1,146,245	1,074,926	1,010,841	884,829	807,192	751,524	708,407	663,418
0.0020	2,945,324	2,529,142	2,240,895	1,968,875	1,704,783	1,432,499	1,336,657	1,251,046	1,084,220	982,528	910,174	854,479	796,708

Table 7-5 Results of Log Pearson Type III Frequency Analyses

Probability	Inflows For Various Percent Confidence That The Inflow Will Not Be Exceeded												
	CL = 99%	CL = 97.5%	CL = 95%	CL = 90%	CL = 80%	CL = 60%	CL = 50%	CL = 40%	CL = 20%	CL = 10%	CL = 5%	CL = 2.5%	CL = 1%
0.0010	3,567,490	3,037,795	2,673,925	2,333,085	2,004,848	1,669,586	1,552,438	1,448,212	1,246,349	1,124,182	1,037,709	971,422	902,933
0.0005	4,263,731	3,602,278	3,151,331	2,731,820	2,330,828	1,924,779	1,783,850	1,658,929	1,418,332	1,273,682	1,171,779	1,093,960	1,013,845
0.0001	6,187,136	5,141,778	4,440,231	3,796,821	3,191,257	2,588,905	2,382,741	2,201,376	1,856,069	1,651,259	1,508,377	1,400,104	1,289,453
Low Inflow Season													
0.5000	68,727	65,878	63,574	61,061	58,198	54,623	53,160	51,736	48,561	46,287	44,462	42,911	41,138
0.2000	139,955	131,575	125,144	118,473	111,284	102,898	99,645	96,576	90,066	85,675	82,306	79,549	76,513
0.1000	207,931	192,620	181,139	169,485	157,226	143,338	138,074	133,174	122,995	116,301	111,264	107,208	102,812
0.0500	290,229	265,260	246,858	228,475	209,477	188,403	180,547	173,303	158,476	148,897	141,785	136,120	130,045
0.0400	320,067	291,342	270,273	249,319	227,768	204,001	195,181	187,069	170,532	159,899	152,032	145,783	139,102
0.0250	388,659	350,886	323,437	296,368	268,789	238,708	227,642	217,513	197,019	183,960	174,362	166,780	158,715
0.0200	424,091	381,448	350,586	320,264	289,499	256,103	243,863	232,684	210,139	195,828	185,340	177,074	168,302
0.0100	546,819	486,453	443,268	401,289	359,189	314,108	297,761	282,918	253,258	234,632	221,091	210,485	199,300
0.0050	690,367	607,903	549,521	493,307	437,513	378,485	357,283	338,130	300,165	276,549	259,496	246,215	232,282
0.0020	916,000	796,528	712,991	633,460	555,491	474,173	445,288	419,355	368,429	337,098	314,656	297,288	279,181
0.0010	1,117,030	962,759	855,816	754,796	656,598	555,188	519,441	487,483	425,124	387,048	359,923	339,023	317,321
0.0005	1,347,193	1,151,399	1,016,766	890,518	768,770	644,191	600,590	561,764	486,453	440,790	408,423	383,584	357,892
0.0001	1,999,908	1,678,991	1,462,024	1,261,661	1,071,627	880,862	815,089	756,991	645,681	579,164	532,504	496,990	460,544

Table 7-6 Parameters Used in Log Pearson Type III Distribution

Season	Mean	Standard Deviation	Skew	Weighted Slew
All	5.12	0.383	-0.194	0.223
High	5.11	0.387	-0.184	-0.216
Low	4.72	0.325	0.0645	-0.0323

Weighted skew is a function of the generalized skew (-0.3000) and Mean Square Error of Generalized Skew (see p. 13, of Bulletin 17B)

Table 7-7 Inflow Ranges (Bins) and Confidence Limit Probabilities for the High Inflow Season - Year 2000

Bin #	LN (Lower Value)	LN (Upper Value)	Lower Value	Upper Value	Designated Bin Value ⁽¹⁾	50% Confidence Limit		80% Confidence Limit		20% Confidence Limit		95% Confidence Limit		5% Confidence Limit	
						Proabability of Exceedence	Probability of Being in Bin	Proabability of Exceedence	Probability of Being in Bin	Proabability of Exceedence	Probability of Being in Bin	Proabability of Exceedence	Probability of Being in Bin	Proabability of Exceedence	Probability of Being in Bin
			0	30,045		1.000		1.000		1.000		1.000		1.000	
1	10.310438	10.581243	30,045	39,389	34,717	0.940	0.060	1.000	0.000	1.000	0.000	1.000	0.000	1.000	0.000
2	10.581243	10.852048	39,389	51,640	45,514	0.865	0.072	0.970	0.030	1.000	0.010	1.000	0.000	0.970	0.030
3	10.852048	11.122853	51,640	67,701	59,670	0.780	0.084	0.911	0.059	1.000	0.025	1.000	0.000	0.920	0.050
4	11.122853	11.393658	67,701	88,757	78,229	0.685	0.095	0.817	0.094	0.900	0.060	0.830	0.100	0.840	0.080
5	11.393658	11.664463	88,757	116,362	102,560	0.565	0.105	0.673	0.144	0.800	0.100	0.680	0.150	0.735	0.105
6	11.664463	11.935268	116,362	152,553	134,458	0.445	0.113	0.498	0.175	0.650	0.154	0.530	0.220	0.617	0.118
7	11.935268	12.206073	152,553	200,000	176,277	0.353	0.121	0.299	0.190	0.402	0.174	0.248	0.220	0.490	0.127
8	12.206073	12.476878	200,000	262,204	231,102	0.225	0.120	0.174	0.125	0.284	0.180	0.138	0.150	0.360	0.130
9	12.476878	12.747683	262,204	343,754	302,979	0.130	0.095	0.103	0.080	0.168	0.116	0.078	0.082	0.235	0.125
10	12.747683	13.018488	343,754	450,669	397,212	0.076	0.060	0.053	0.051	0.106	0.075	0.036	0.042	0.145	0.090
11	13.018488	13.289293	450,669	590,835	520,752	0.038	0.038	0.023	0.030	0.060	0.046	0.014	0.022	0.085	0.060
12	13.289293	13.560098	590,835	774,597	682,716	0.017	0.021	0.009	0.014	0.030	0.030	0.004	0.010	0.047	0.038
13	13.560098	13.830903	774,597	1,015,511	895,054	0.006	0.011	0.003	0.006	0.014	0.016	0.001	0.003	0.025	0.023
14	13.830903	14.101708	1,015,511	1,331,355	1,173,433	0.002	0.004	0.001	0.002	0.005	0.008	0.0002460	0.001	0.012	0.013
15	14.101708	14.372513	1,331,355	1,745,432	1,538,394	0.001	0.002	0.000	0.001	0.002	0.003	0.0000415	0.000	0.005	0.007
16	14.372513	14.643318	1,745,432	2,288,296	2,016,864	0.000	0.000	0.000	0.000	0.001	0.001	0.0000044	0.000	0.002	0.003
17	14.643318	14.914123	2,288,296	3,000,000	2,644,148	0.000	0.000	0.000	0.000	0.000	0.000	0.0000005	0.000	0.001	0.001
						Totals =	1.000		1.000		0.9994		0.9998		0.9994

⁽¹⁾ Designated Bin Value is average of Lower & Upper Value.

Table 7-8 Results of Logistic Regressions

River	a (Slope)	b (Intercept)	r ²	Standard Error of Regression
Sacramento + Yolo Bypass	.563	-5.21	0.054	0.530
San Joaquin River	0.430	-4.173	0.075	0.709
Miscellaneous Flows	0.379	-4.453	0.071	0.665
Cosumnes River	1.116	-9.670	0.358	0.714

Table 7-9 Historic Island/Tract Breaches Since 1900

	Location		Years	No. Of Failures
1	Bacon	Island	1938	1
2	Big Break	Island	1927	1
3	Bishop	Tract	1904	1
4	Brack	Tract	1904	1
5	Byron	Tract	1907	1
6	Coney	Island	1907	1
7	Donlon	Island	1937	1
8	Edgerly	Island	1983	1
9	Grand	Island	1955	1
10	Holland	Tract	1980	1
11	Honker Bay Club	Island	2006	1
12	Little Holland	Tract	1963	1
13	Lower Roberts	Island	1906	1
14	Mandeville	Island	1938	1
15	Mc Donald	Island	1982	1
16	Medford	Island	1936	1
17	Palm	Tract	1907	1
18	Rd 1007	Tract	1925	1
19	Shima	Tract	1983	1
20	Union	Island	1906	1
21	Upper Jones	Tract	2004	1
22	Upper Roberts	Tract	1950	1
23	Walthall	Tract	1997	1
24	Wetherbee	Lake	1997	1
25	Bradford	Island	1950-1983	2
26	Cliftoncourt	Tract	1901-1907	2
27	Empire	Tract	1950-1955	2
28	Fabian	Tract	1901-1906	2
29	Fay	Island	1983-2006	2
30	Glanville	Island	1986-1997	2
31	Grizzly	Island	1983-1998	2

Table 7-9 Historic Island/Tract Breaches Since 1900

	Location		Years	No. Of Failures
32	Ida	Island	1950-1955	2
33	McMullin Ranch	Tract	1997-1950	2
34	Middle Roberts	Island	1920-1938	2
35	Rhode	Island	1938-1971	2
36	Sargent Barnhart	Tract	1904-1907	2
37	Simmons Wheeler	Island	2005-2006	2
36	Staten	Island	1904-1907	2
37	Terminus	Tract	1907-1958	2
38	Victoria	Island	1901-1907	2
39	Webb	Tract	1950-1980	2
40	Little Mandeville	Island	1980-1986-1994	3
41	Ryer	Island	1904-1907-1986	3
42	Franks	Tract	1907-1936-1938	3
43	Little Franks	Tract	1981-1982-1983	3
44	Lower Jones	Tract	1906-1907-1980-2004*	3
45	Mildred	Island	1965-1969-1983	3
46	Mossdale Rd17	Tract	1901-1911-1950	3
47	Paradise	Junction	1920-1950-1997	3
48	Pescadero	Tract	1938-1950-1997	3
49	River Junction	Junction	1958-1983-1997	3
50	Stewart	Tract	1938-1950-1997	3
51	Twitchell	Island	1906-1907-1908	3
52	Tyler	Island	1904-1907-1986	3
53	Van Sickle	Island	1983-1998-2006	3
54	Bethel	Island	1907-1908-1909-1911	4
55	Bouldin	Island	1904-1907-1908-1909	4
56	Jersey	Island	1900-1904-1907-1909	4
57	Quimby	Island	1936-1938-1950-1955	4
58	Shin Kee	Tract	1938-1958-1965-1986	4
59	Brannan-Andrus	Island	1902-1904-1907-1909-1972	5
60	Sherman	Island	1904-1906-1909-1937-1969	5
61	Dead Horse	Island	1950-1955-1958-1980-1986-1997	6
62	Mc Cormack-Williamson	Tract	1938-1950-1955-1958-1964-1986-1997	7
63	New Hope	Tract	1900-1904-1907-1928-1950-1955-1986	7
64	Prospect	Island	1963-1980-1981-1982-1983-1986-1995-1997	8
65	Venice	Island	1904-1906-1907-1909-1932-1938-1950-1982	8
Number Of Island/Tract Breaches				166

Table 7-10 Vulnerability Classes Considered for Underseepage Analyses

Geographic Region	Vulnerability Class Index	Peat Thickness (ft)	Slough Width	Random Input Variables
Delta	1	0	Narrow	Ditch, Sediment
	2	0	Not Narrow	Ditch, Sediment
	3	0.1-5	Narrow	Ditch, Sediment, Peat Thickness, Peat Permeability
	4	0.1-5	Not Narrow	Ditch, Sediment, Peat Thickness, Peat Permeability
	5	5.1-10	Narrow	Ditch, Sediment, Peat Thickness, Peat Permeability
	6	5.1-10	Not Narrow	Ditch, Sediment, Peat Thickness, Peat Permeability
	7	10.1-15	Narrow	Ditch, Sediment, Peat Thickness, Peat Permeability
	8	10.1-15	Not Narrow	Ditch, Sediment, Peat Thickness, Peat Permeability
	9	15.1-30	Narrow	Ditch, Sediment, Peat Thickness, Peat Permeability
	10	15.1-30	Not Narrow	Ditch, Sediment, Peat Thickness, Peat Permeability
	11	>30	Narrow	Ditch, Sediment, Peat Thickness, Peat Permeability
	12	>30	Not Narrow	Ditch, Sediment, Peat Thickness, Peat Permeability
Suisan Marsh	13	0	Narrow	Sediment
	14	0	Not Narrow	Sediment
	15	0.1-5	Narrow	Sediment, Peat Thickness, Peat Permeability
	16	0.1-5	Not Narrow	Sediment, Peat Thickness, Peat Permeability
	17	5.1-10	Narrow	Sediment, Peat Thickness, Peat Permeability
	18	5.1-10	Not Narrow	Sediment, Peat Thickness, Peat Permeability
	19	10.1-15	Narrow	Sediment, Peat Thickness, Peat Permeability
	20	10.1-15	Not Narrow	Sediment, Peat Thickness, Peat Permeability
	21	15.1-30	Narrow	Sediment, Peat Thickness, Peat Permeability
	22	15.1-30	Not Narrow	Sediment, Peat Thickness, Peat Permeability
	23	>30	Narrow	Sediment, Peat Thickness, Peat Permeability
	24	>30	Not Narrow	Sediment, Peat Thickness, Peat Permeability

Table 7-11 Distribution of Probability of Failure – Sample Results

Analysis Zone ID	Island/Tract Name	Reach ID	V Class	Reach Crest EL	Reach WSE	Reach Free board	Mean of Ln P _f *	Std Dev of Ln P _f *	Confidence Level*										
									1%	10%	20%	30%	40%	50%	60%	70%	80%	90%	100%
4	Webb_Tract	004001	10	10.7	4.482	6.177	-2.378	0.885	0.012	0.030	0.044	0.058	0.074	0.093	0.116	0.148	0.195	0.288	0.908
4	Webb_Tract	004002	9	10.8	4.482	6.367	-2.742	0.929	0.007	0.020	0.029	0.040	0.051	0.064	0.082	0.105	0.141	0.212	0.705
4	Webb_Tract	004003	7	10.6	4.483	6.093	-2.050	0.839	0.018	0.044	0.064	0.083	0.104	0.129	0.159	0.200	0.261	0.377	1.000
4	Webb_Tract	004004	7	11.7	4.484	7.225	-2.286	0.839	0.014	0.035	0.050	0.065	0.082	0.102	0.126	0.158	0.206	0.298	0.882
4	Webb_Tract	004005	7	11.2	4.485	6.668	-2.170	0.839	0.016	0.039	0.056	0.074	0.092	0.114	0.141	0.177	0.231	0.335	0.991
4	Webb_Tract	004006	7	10.7	4.486	6.217	-2.076	0.839	0.018	0.043	0.062	0.081	0.101	0.125	0.155	0.195	0.254	0.368	1.000
4	Webb_Tract	004007	8	10.2	4.487	5.684	-1.639	0.771	0.032	0.072	0.101	0.130	0.160	0.194	0.236	0.291	0.371	0.521	1.000
4	Webb_Tract	004008	10	10.1	4.488	5.615	-2.262	0.885	0.013	0.033	0.049	0.065	0.083	0.104	0.130	0.166	0.219	0.324	1.000
4	Webb_Tract	004009	10	11.2	4.488	6.726	-2.491	0.885	0.011	0.027	0.039	0.052	0.066	0.083	0.104	0.132	0.175	0.258	0.811
4	Webb_Tract	004010	10	10.3	4.488	5.849	-2.310	0.885	0.013	0.032	0.047	0.062	0.079	0.099	0.124	0.158	0.209	0.309	0.971
4	Webb_Tract	004011	10	10.2	4.473	5.721	-2.284	0.885	0.013	0.033	0.048	0.064	0.081	0.102	0.128	0.162	0.215	0.317	0.997
4	Webb_Tract	004012	10	10.1	4.469	5.673	-2.274	0.885	0.013	0.033	0.049	0.065	0.082	0.103	0.129	0.164	0.217	0.320	1.000
4	Webb_Tract	004013	10	9.7	4.472	5.267	-2.190	0.885	0.014	0.036	0.053	0.070	0.089	0.112	0.140	0.178	0.236	0.348	1.000
4	Webb_Tract	004014	10	10.5	4.477	5.986	-2.338	0.885	0.012	0.031	0.046	0.061	0.077	0.096	0.121	0.153	0.203	0.300	0.944
4	Webb_Tract	004015	10	10.1	4.478	5.661	-2.272	0.885	0.013	0.033	0.049	0.065	0.082	0.103	0.129	0.164	0.217	0.321	1.000
4	Webb_Tract	004016	10	10.0	4.484	5.486	-2.236	0.885	0.014	0.034	0.051	0.067	0.085	0.107	0.134	0.170	0.225	0.333	1.000
4	Webb_Tract	004017	10	10.0	4.483	5.537	-2.246	0.885	0.013	0.034	0.050	0.067	0.085	0.106	0.132	0.168	0.223	0.329	1.000
4	Webb_Tract	004018	10	10.0	4.481	5.523	-2.243	0.885	0.014	0.034	0.050	0.067	0.085	0.106	0.133	0.169	0.224	0.330	1.000
4	Webb_Tract	004019	10	9.8	4.456	5.334	-2.204	0.885	0.014	0.035	0.052	0.069	0.088	0.110	0.138	0.176	0.233	0.343	1.000
4	Webb_Tract	004020	10	10.0	4.441	5.539	-2.246	0.885	0.013	0.034	0.050	0.066	0.085	0.106	0.132	0.168	0.223	0.329	1.000
4	Webb_Tract	004021	10	10.4	4.459	5.929	-2.327	0.885	0.012	0.031	0.046	0.061	0.078	0.098	0.122	0.155	0.206	0.304	0.955

SECTION SEVEN

Flood Risk Analysis

Table 7-11 Distribution of Probability of Failure – Sample Results

Analysis Zone ID	Island/Tract Name	Reach ID	V Class	Reach Crest EL	Reach WSE	Reach Free board	Mean of Ln P _f *	Std Dev of Ln P _f *	Confidence Level*										
									1%	10%	20%	30%	40%	50%	60%	70%	80%	90%	100%
4	Webb_Tract	004022	10	10.6	4.463	6.151	-2.372	0.885	0.012	0.030	0.044	0.059	0.075	0.093	0.117	0.148	0.196	0.290	0.912
4	Webb_Tract	004023	10	12.0	4.466	7.527	-2.656	0.885	0.009	0.023	0.033	0.044	0.056	0.070	0.088	0.112	0.148	0.218	0.687
4	Webb_Tract	004024	10	11.0	4.469	6.496	-2.443	0.885	0.011	0.028	0.041	0.055	0.069	0.087	0.109	0.138	0.183	0.270	0.850
4	Webb_Tract	004025	12	10.9	4.468	6.430	-4.279	0.995	0.001	0.004	0.006	0.008	0.011	0.014	0.018	0.023	0.032	0.050	0.180
4	Webb_Tract	004026	12	11.2	4.473	6.719	-4.317	0.995	0.001	0.004	0.006	0.008	0.010	0.013	0.017	0.022	0.031	0.048	0.173
4	Webb_Tract	004027	10	11.1	4.475	6.659	-2.477	0.885	0.011	0.027	0.040	0.053	0.067	0.084	0.105	0.134	0.177	0.261	0.822
4	Webb_Tract	004028	10	10.5	4.476	6.011	-2.344	0.885	0.012	0.031	0.046	0.060	0.077	0.096	0.120	0.153	0.202	0.299	0.939
4	Webb_Tract	004029	10	10.9	4.477	6.460	-2.436	0.885	0.011	0.028	0.042	0.055	0.070	0.088	0.110	0.139	0.184	0.272	0.856
4	Webb_Tract	004030	8	11.1	4.477	6.656	-1.836	0.771	0.027	0.059	0.083	0.106	0.131	0.159	0.194	0.239	0.305	0.428	1.000
4	Webb_Tract	004031	8	10.2	4.475	5.679	-1.638	0.771	0.032	0.072	0.102	0.130	0.160	0.194	0.236	0.291	0.372	0.522	1.000
4	Webb_Tract	004032	10	11.0	4.471	6.542	-2.453	0.885	0.011	0.028	0.041	0.054	0.069	0.086	0.108	0.137	0.181	0.268	0.842
4	Webb_Tract	004033	10	11.1	4.460	6.592	-2.463	0.885	0.011	0.027	0.040	0.054	0.068	0.085	0.107	0.135	0.179	0.265	0.833
4	Webb_Tract	004034	10	11.1	4.467	6.667	-2.479	0.885	0.011	0.027	0.040	0.053	0.067	0.084	0.105	0.133	0.177	0.261	0.821
4	Webb_Tract	004035	8	10.7	4.481	6.255	-1.755	0.771	0.029	0.064	0.090	0.115	0.142	0.173	0.210	0.259	0.331	0.464	1.000
4	Webb_Tract	004036	10	10.6	4.482	6.140	-2.370	0.885	0.012	0.030	0.044	0.059	0.075	0.093	0.117	0.149	0.197	0.291	0.915
4	Webb_Tract	004037	10	11.2	4.484	6.755	-2.497	0.885	0.010	0.026	0.039	0.052	0.066	0.082	0.103	0.131	0.174	0.256	0.806
4	Webb_Tract	004038	10	10.1	4.487	5.659	-2.271	0.885	0.013	0.033	0.049	0.065	0.082	0.103	0.129	0.164	0.217	0.321	1.000
4	Webb_Tract	004039	10	10.5	4.487	6.063	-2.354	0.885	0.012	0.031	0.045	0.060	0.076	0.095	0.119	0.151	0.200	0.295	0.929
4	Webb_Tract	004040	8	10.6	4.484	6.092	-1.722	0.771	0.030	0.067	0.093	0.119	0.147	0.179	0.217	0.268	0.342	0.480	1.000
4	Webb_Tract	004041	6	10.8	4.482	6.312	-2.314	0.845	0.014	0.033	0.049	0.063	0.080	0.099	0.122	0.154	0.201	0.292	0.871
4	Webb_Tract	004042	10	11.3	4.487	6.804	-2.507	0.885	0.010	0.026	0.039	0.051	0.065	0.082	0.102	0.130	0.172	0.254	0.798

Table 7-11 Distribution of Probability of Failure – Sample Results

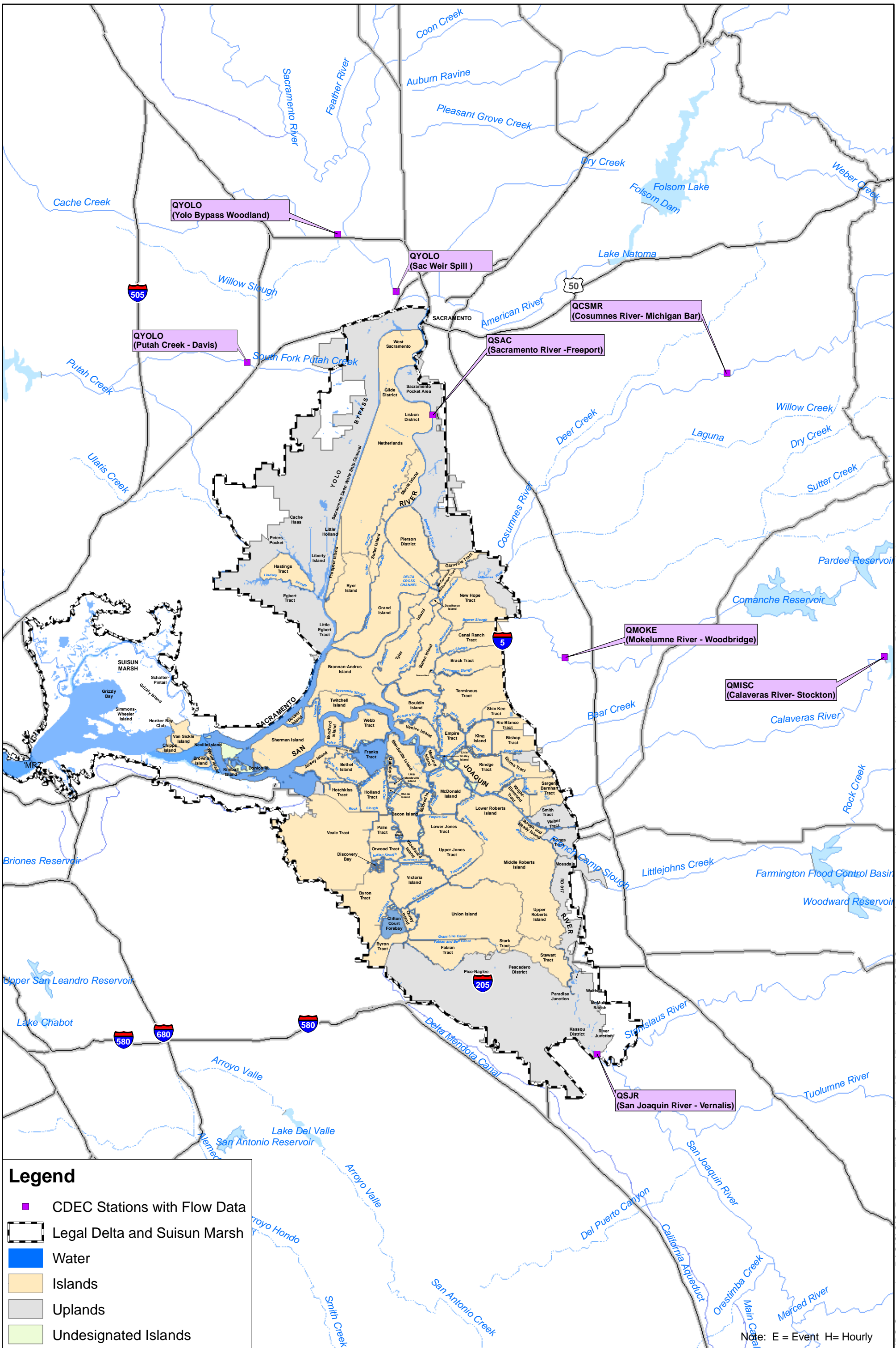
Analysis Zone ID	Island/Tract Name	Reach ID	V Class	Reach Crest EL	Reach WSE	Reach Free board	Mean of Ln P _f *	Std Dev of Ln P _f *	Confidence Level*										
									1%	10%	20%	30%	40%	50%	60%	70%	80%	90%	100%
4	Webb_Tract	004043	10	10.8	4.488	6.291	-2.401	0.885	0.012	0.029	0.043	0.057	0.072	0.091	0.113	0.144	0.191	0.282	0.887
4	Webb_Tract	004044	10	11.1	4.486	6.624	-2.470	0.885	0.011	0.027	0.040	0.053	0.068	0.085	0.106	0.135	0.178	0.263	0.828
4	Webb_Tract	004045	10	10.6	4.484	6.123	-2.367	0.885	0.012	0.030	0.045	0.059	0.075	0.094	0.117	0.149	0.198	0.292	0.918
4	Webb_Tract	004046	10	10.2	4.484	5.668	-2.273	0.885	0.013	0.033	0.049	0.065	0.082	0.103	0.129	0.164	0.217	0.320	1.000
4	Webb_Tract	004047	10	10.2	4.485	5.751	-2.290	0.885	0.013	0.033	0.048	0.064	0.081	0.101	0.127	0.161	0.213	0.315	0.991
4	Webb_Tract	004048	10	10.5	4.486	6.024	-2.346	0.885	0.012	0.031	0.045	0.060	0.076	0.096	0.120	0.152	0.202	0.298	0.937
4	Webb_Tract	004049	10	11.3	4.487	6.799	-2.506	0.885	0.010	0.026	0.039	0.051	0.065	0.082	0.102	0.130	0.172	0.254	0.799
4	Webb_Tract	004050	8	11.4	4.486	6.952	-1.896	0.771	0.025	0.056	0.078	0.100	0.123	0.150	0.182	0.225	0.287	0.403	1.000
4	Webb_Tract	004051	8	11.3	4.483	6.833	-1.872	0.771	0.026	0.057	0.080	0.103	0.126	0.154	0.187	0.230	0.294	0.413	1.000
4	Webb_Tract	004052	10	11.4	4.482	6.968	-2.541	0.885	0.010	0.025	0.037	0.050	0.063	0.079	0.099	0.125	0.166	0.245	0.771
4	Webb_Tract	004053	8	10.8	4.481	6.285	-1.761	0.771	0.029	0.064	0.090	0.115	0.141	0.172	0.209	0.257	0.329	0.461	1.000
4	Webb_Tract	004054	8	10.4	4.482	5.873	-1.678	0.771	0.031	0.070	0.098	0.125	0.154	0.187	0.227	0.280	0.357	0.502	1.000
4	Webb_Tract	004055	8	10.9	4.482	6.378	-1.780	0.771	0.028	0.063	0.088	0.113	0.139	0.169	0.205	0.253	0.323	0.453	1.000
4	Webb_Tract	004056	8	10.1	4.481	5.589	-1.620	0.771	0.033	0.074	0.103	0.132	0.163	0.198	0.241	0.296	0.379	0.531	1.000
4	Webb_Tract	004057	10	10.0	4.480	5.565	-2.252	0.885	0.013	0.034	0.050	0.066	0.084	0.105	0.132	0.167	0.222	0.327	1.000
4	Webb_Tract	004058	10	10.1	4.476	5.631	-2.265	0.885	0.013	0.033	0.049	0.065	0.083	0.104	0.130	0.165	0.219	0.323	1.000
4	Webb_Tract	004059	8	10.2	4.469	5.738	-1.650	0.771	0.032	0.071	0.100	0.128	0.158	0.192	0.233	0.288	0.367	0.516	1.000
4	Webb_Tract	004060	8	10.1	4.464	5.610	-1.624	0.771	0.033	0.073	0.103	0.132	0.162	0.197	0.240	0.295	0.377	0.529	1.000
4	Webb_Tract	004061	8	11.0	4.462	6.524	-1.810	0.771	0.027	0.061	0.086	0.109	0.135	0.164	0.199	0.245	0.313	0.440	1.000
4	Webb_Tract	004062	10	10.6	4.463	6.115	-2.365	0.885	0.012	0.030	0.045	0.059	0.075	0.094	0.118	0.149	0.198	0.292	0.919
4	Webb_Tract	004063	10	12.4	4.462	7.928	-2.738	0.885	0.008	0.021	0.031	0.041	0.052	0.065	0.081	0.103	0.136	0.201	0.633

Table 7-11 Distribution of Probability of Failure – Sample Results

Analysis Zone ID	Island/Tract Name	Reach ID	V Class	Reach Crest EL	Reach WSE	Reach Free board	Mean of Ln P _f *	Std Dev of Ln P _f *	Confidence Level*										
									1%	10%	20%	30%	40%	50%	60%	70%	80%	90%	100%
4	Webb_Tract	004064	10	11.3	4.454	6.828	-2.512	0.885	0.010	0.026	0.038	0.051	0.065	0.081	0.102	0.129	0.171	0.252	0.794
4	Webb_Tract	004065	10	11.1	4.456	6.674	-2.480	0.885	0.011	0.027	0.040	0.053	0.067	0.084	0.105	0.133	0.176	0.260	0.819
4	Webb_Tract	004066	10	12.1	4.462	7.642	-2.679	0.885	0.009	0.022	0.033	0.043	0.055	0.069	0.086	0.109	0.145	0.213	0.671
4	Webb_Tract	004067	10	12.0	4.469	7.534	-2.657	0.885	0.009	0.023	0.033	0.044	0.056	0.070	0.088	0.112	0.148	0.218	0.686
4	Webb_Tract	004068	10	11.4	4.478	6.920	-2.531	0.885	0.010	0.026	0.038	0.050	0.064	0.080	0.100	0.127	0.168	0.248	0.779
4	Webb_Tract	004069	10	10.3	4.478	5.780	-2.296	0.885	0.013	0.032	0.048	0.063	0.080	0.101	0.126	0.160	0.212	0.313	0.985

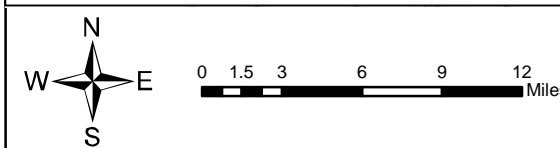
Note: *
Probability of failure calculated for No-Human Intervention Case.

Figures



Legend

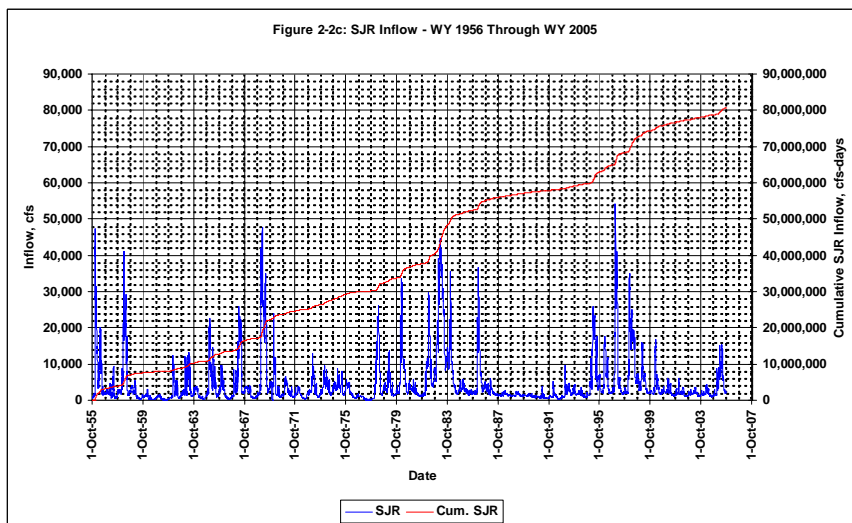
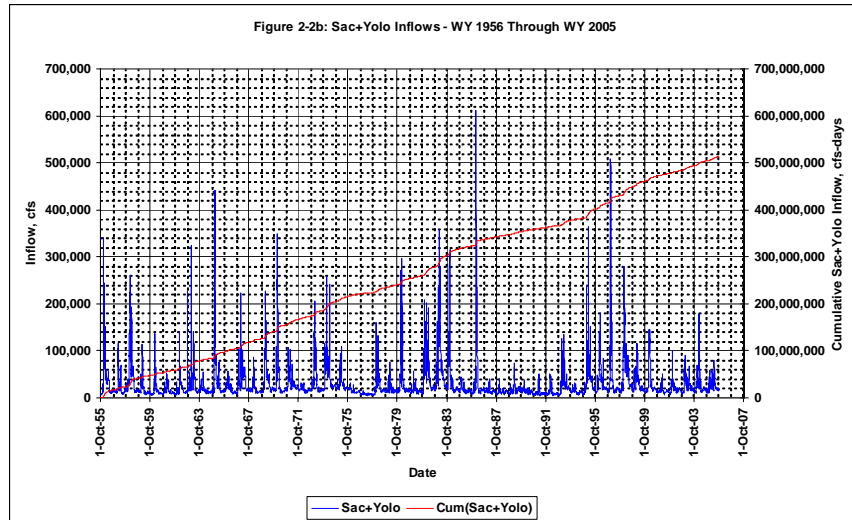
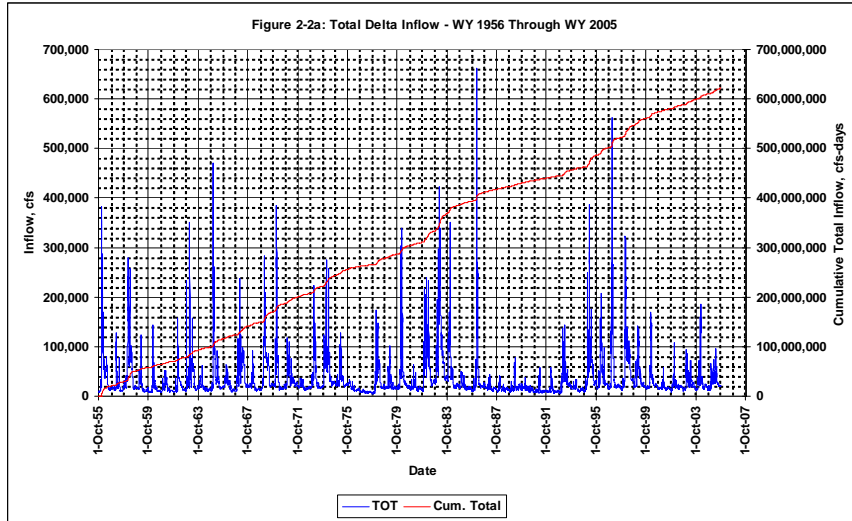
- CDEC Stations with Flow Data
- Legal Delta and Suisun Marsh
- Water
- Islands
- Uplands
- Undesignated Islands



Note: E = Event H= Hourly

URS Corporation P:\GIS\GIS_Project_Files\OriginalData\Regional_Data\CDEC_stations\stations_with_flow_data.mxd Date: 12/11/2006 2:35:15 PM Name: smlewis0

Figure 7-2 Historical Delta Inflows



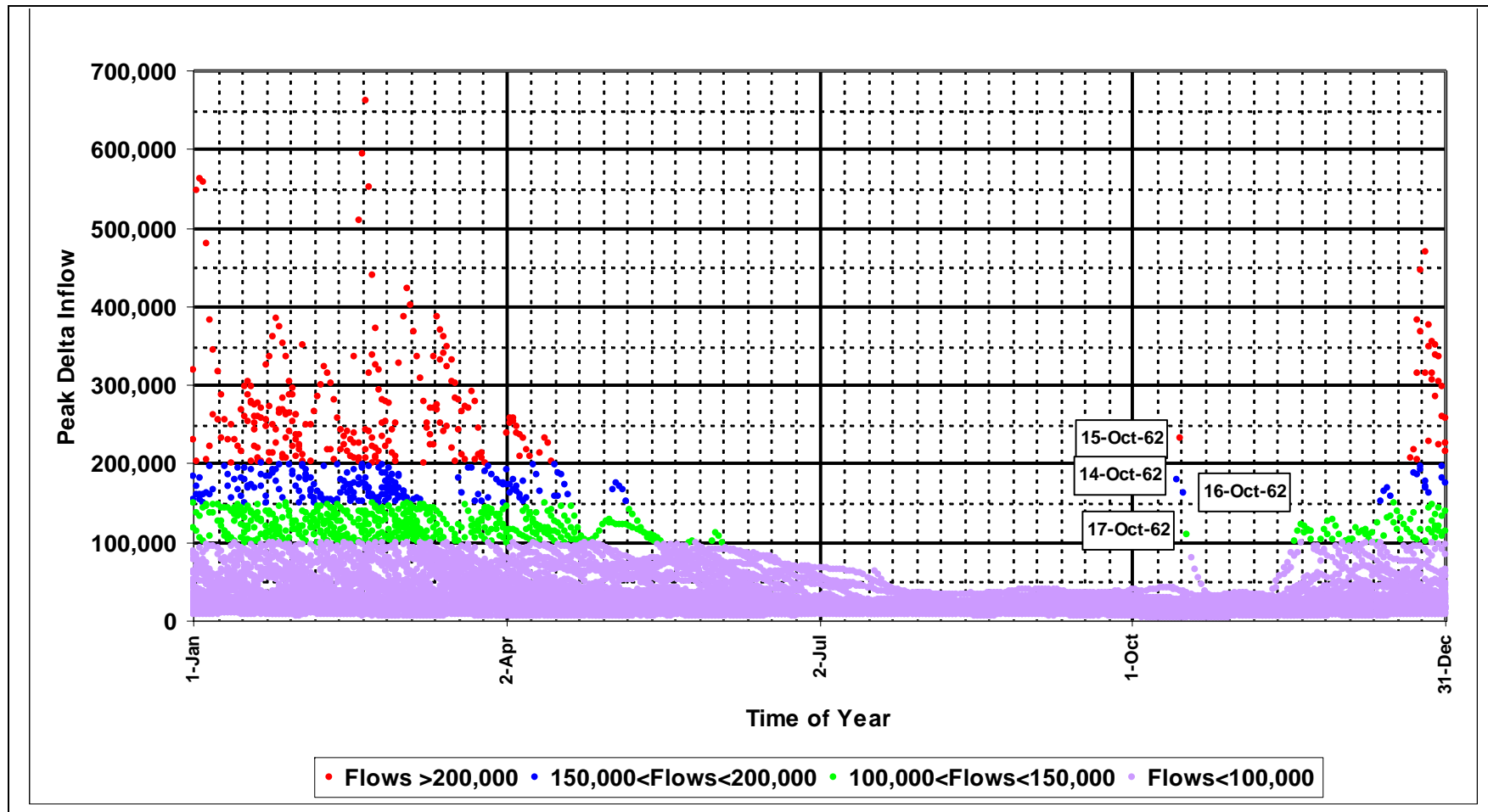


Figure 7-3 Temporal Distribution of Peak Delta Inflows

Figure 7-4: ALL SEASONS FLOW FREQUENCY
(CL = Confidence Limit %)

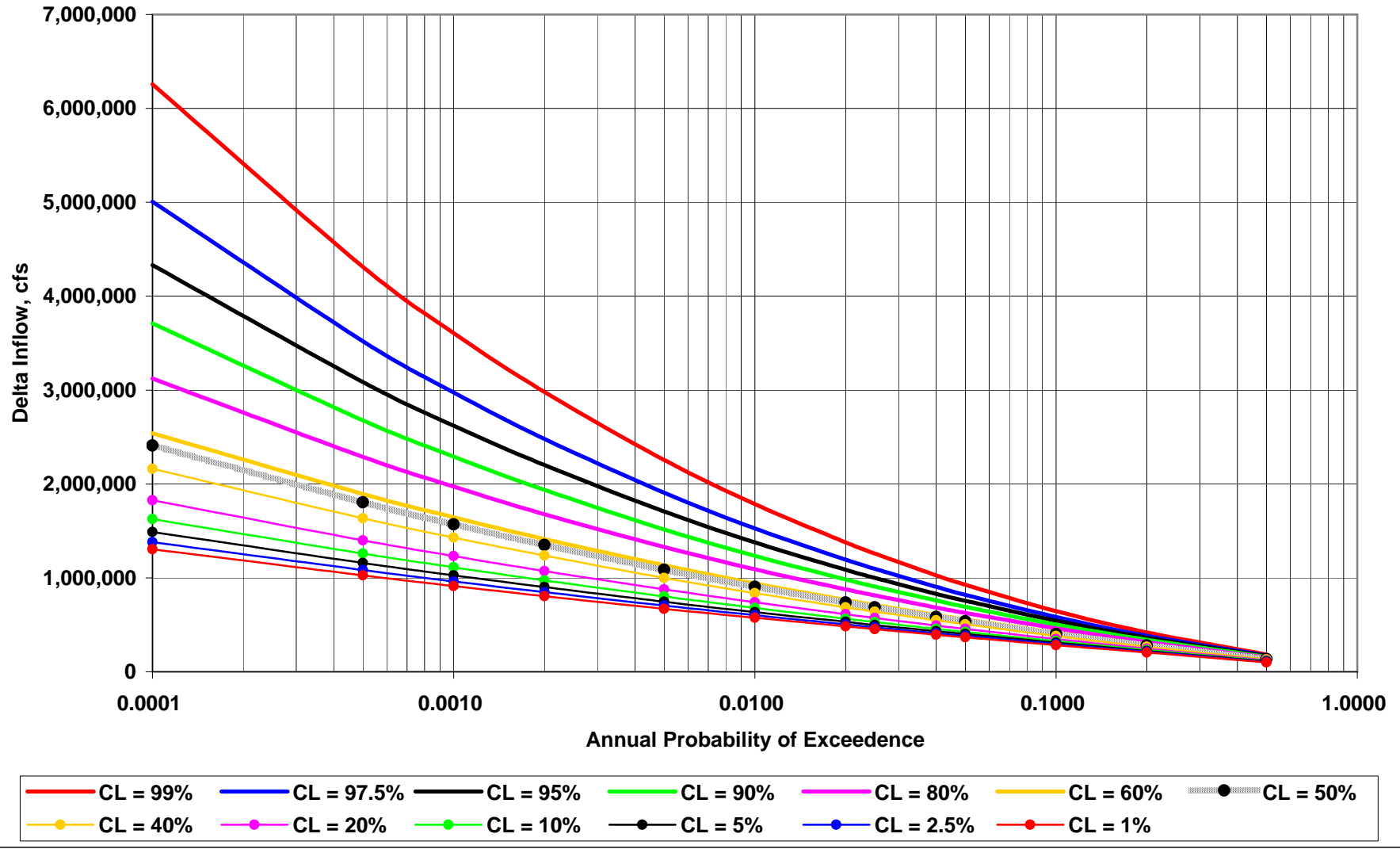


Figure 7-5: HIGH RUNOFF SEASON - INFLOW FREQUENCY
 (CL = Confidence Limit %)

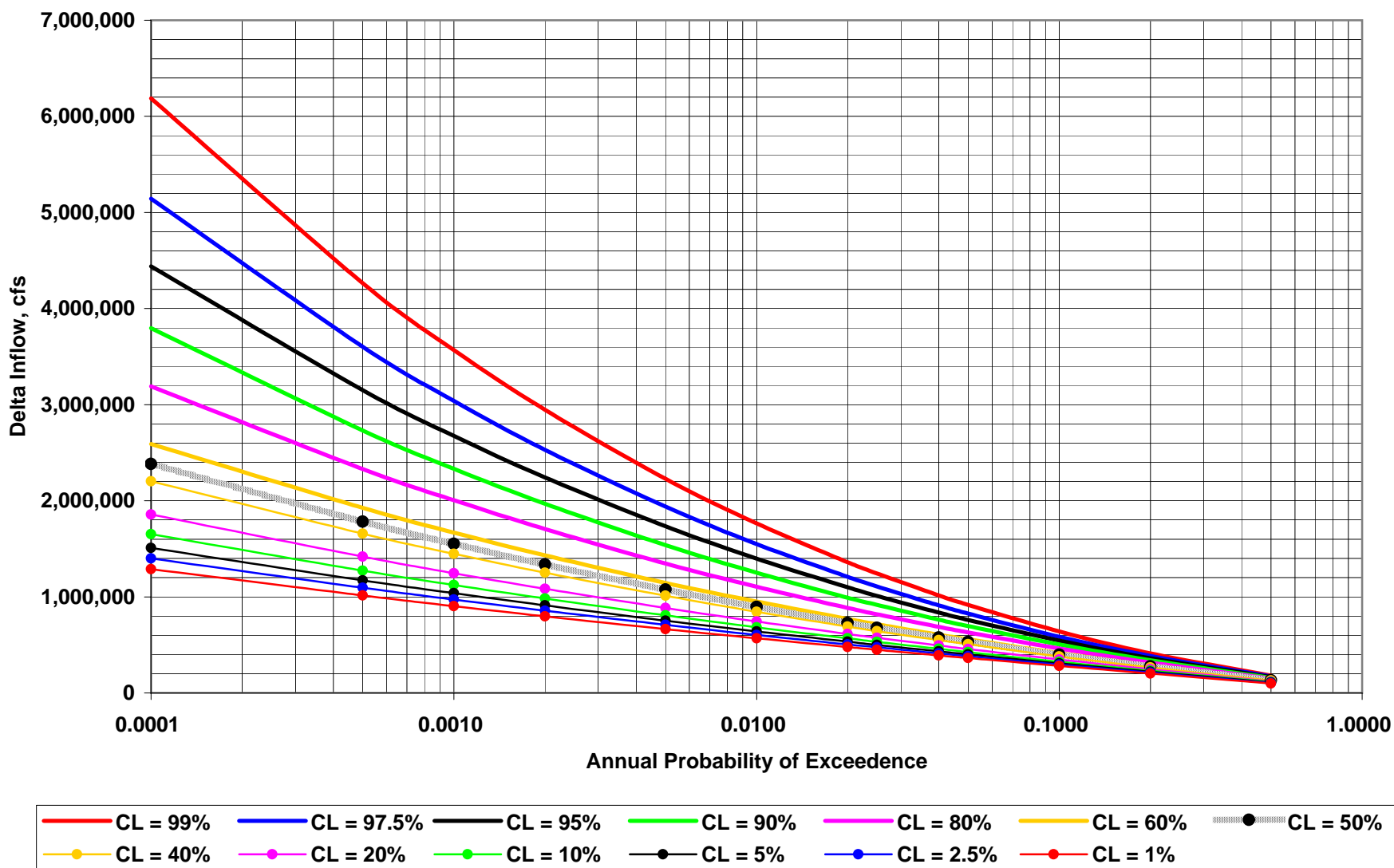


Figure 7-6: LOW RUNOFF SEASON - INFLOW FREQUENCY
 (CL = Confidence Limit %)

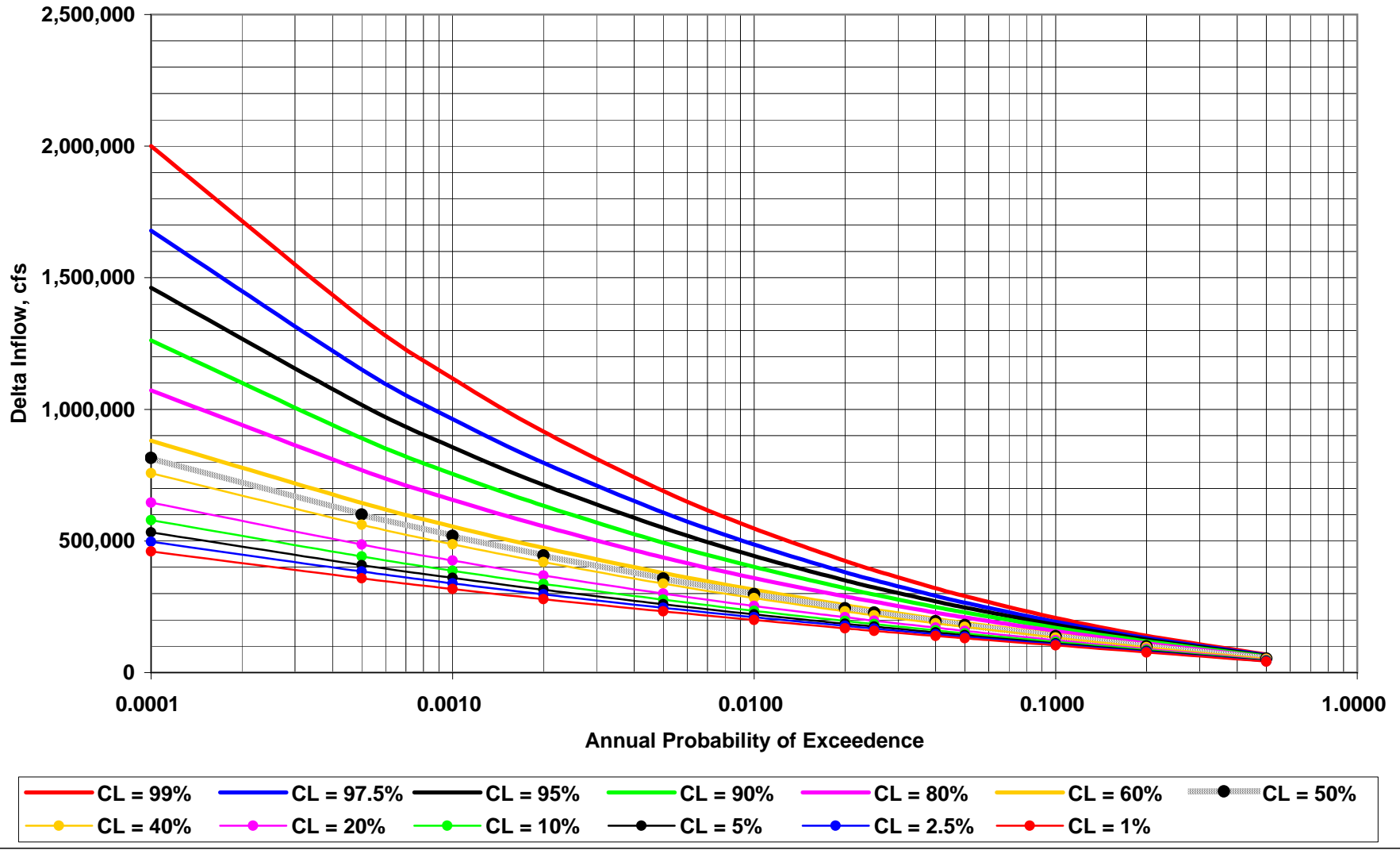
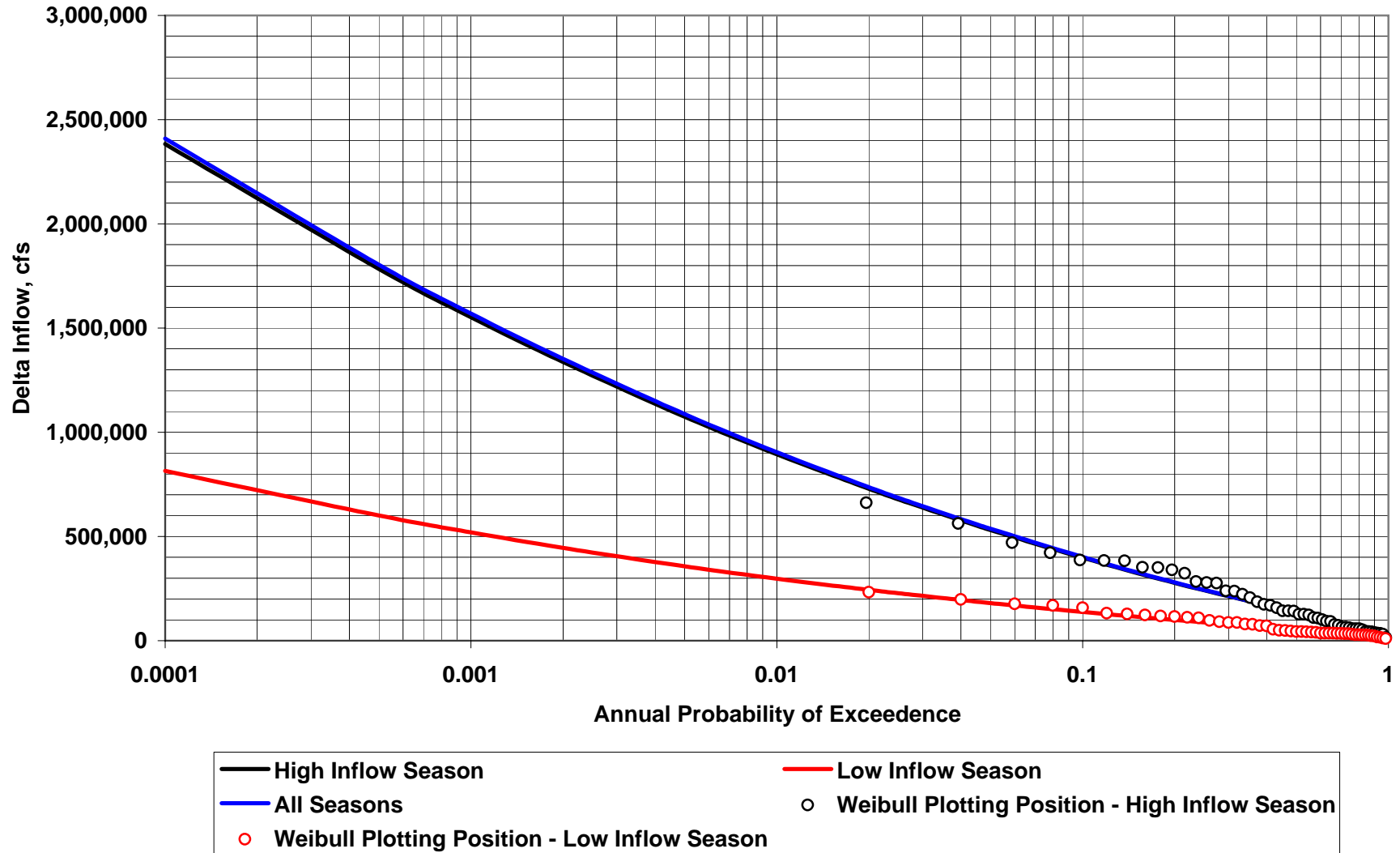


Figure 7-7: COMPARISON BETWEEN INFLOW-FREQUENCY CURVES, CL = 50%
 (CL = Confidence Limit %)



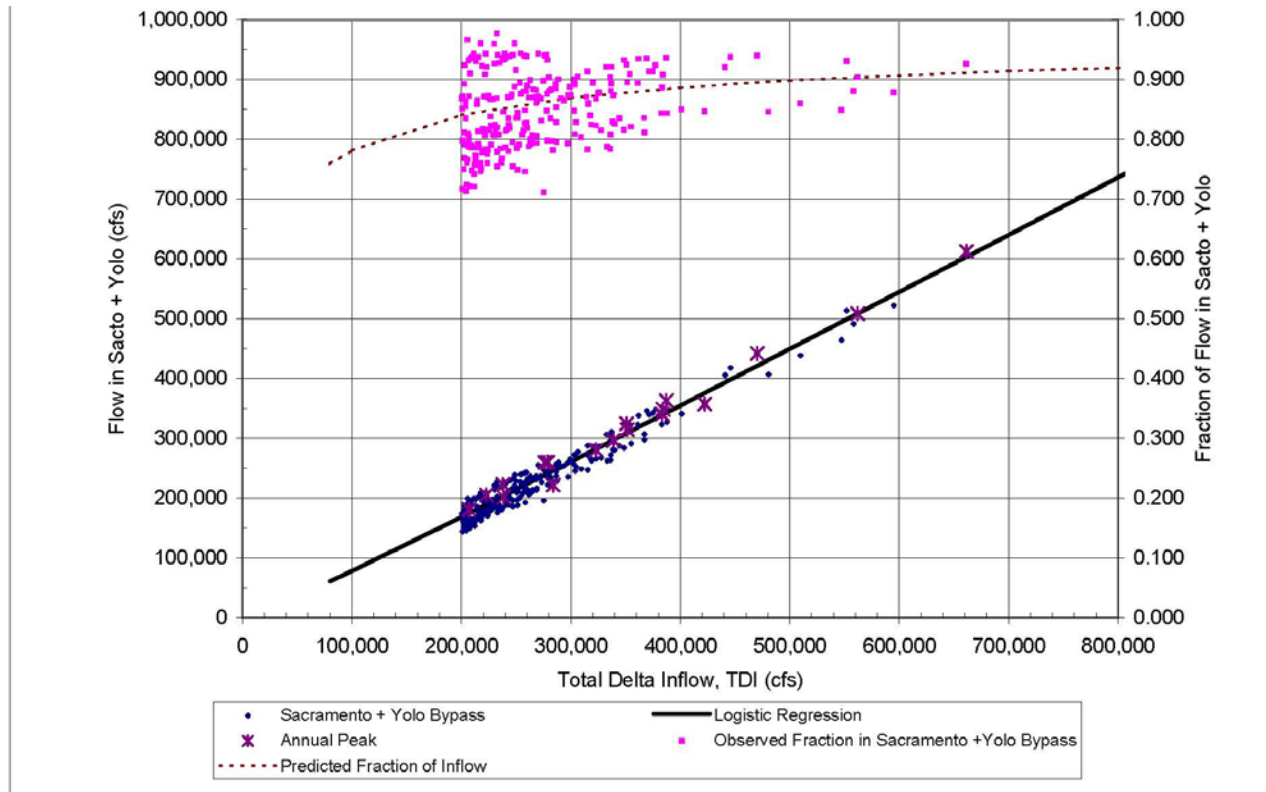


Figure 7-8 Flow in Sacramento River Plus Yolo Bypass Versus Total Delta Inflow

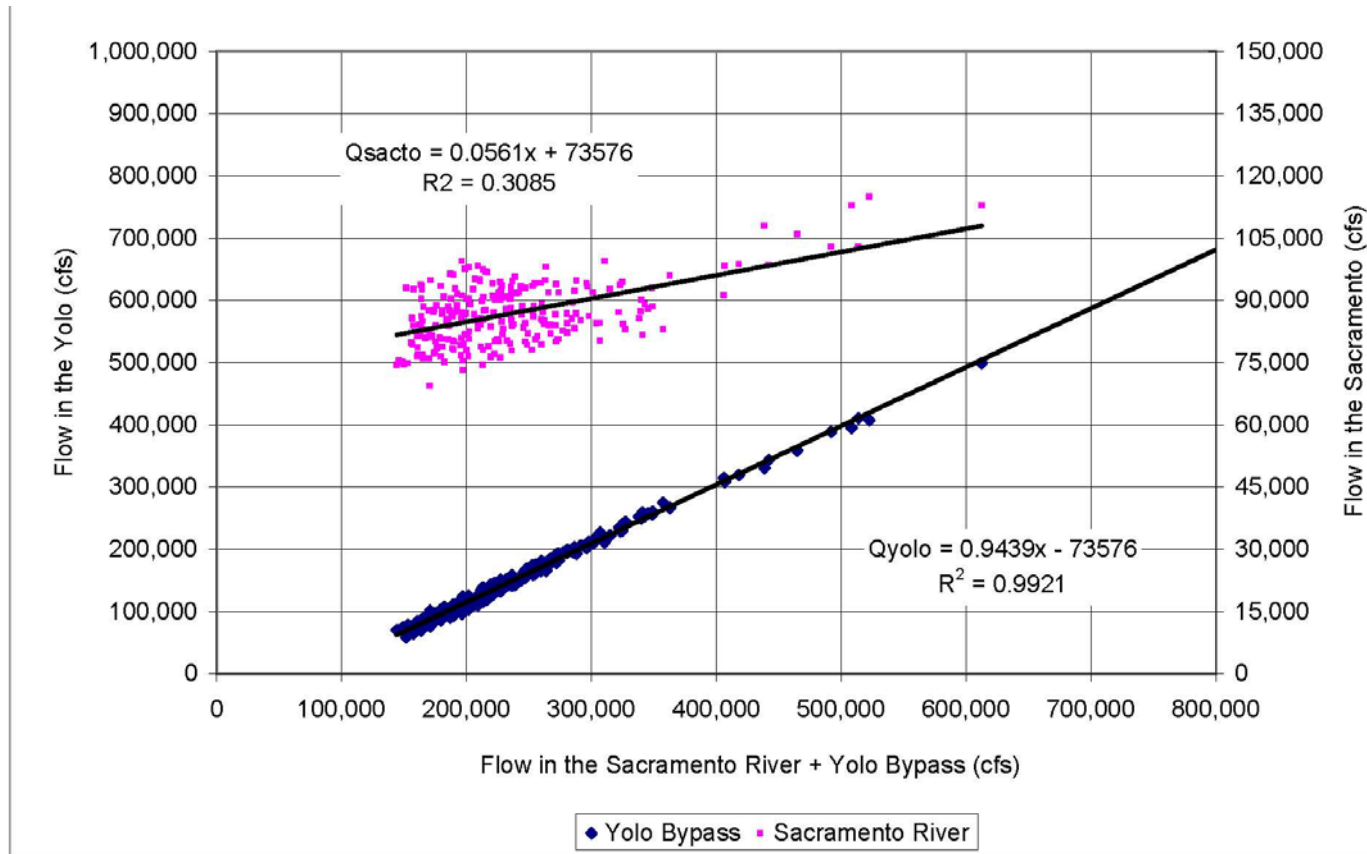


Figure 7-9 Relationship Between Flow in Yolo Bypass and Total Flow in the Sacramento River

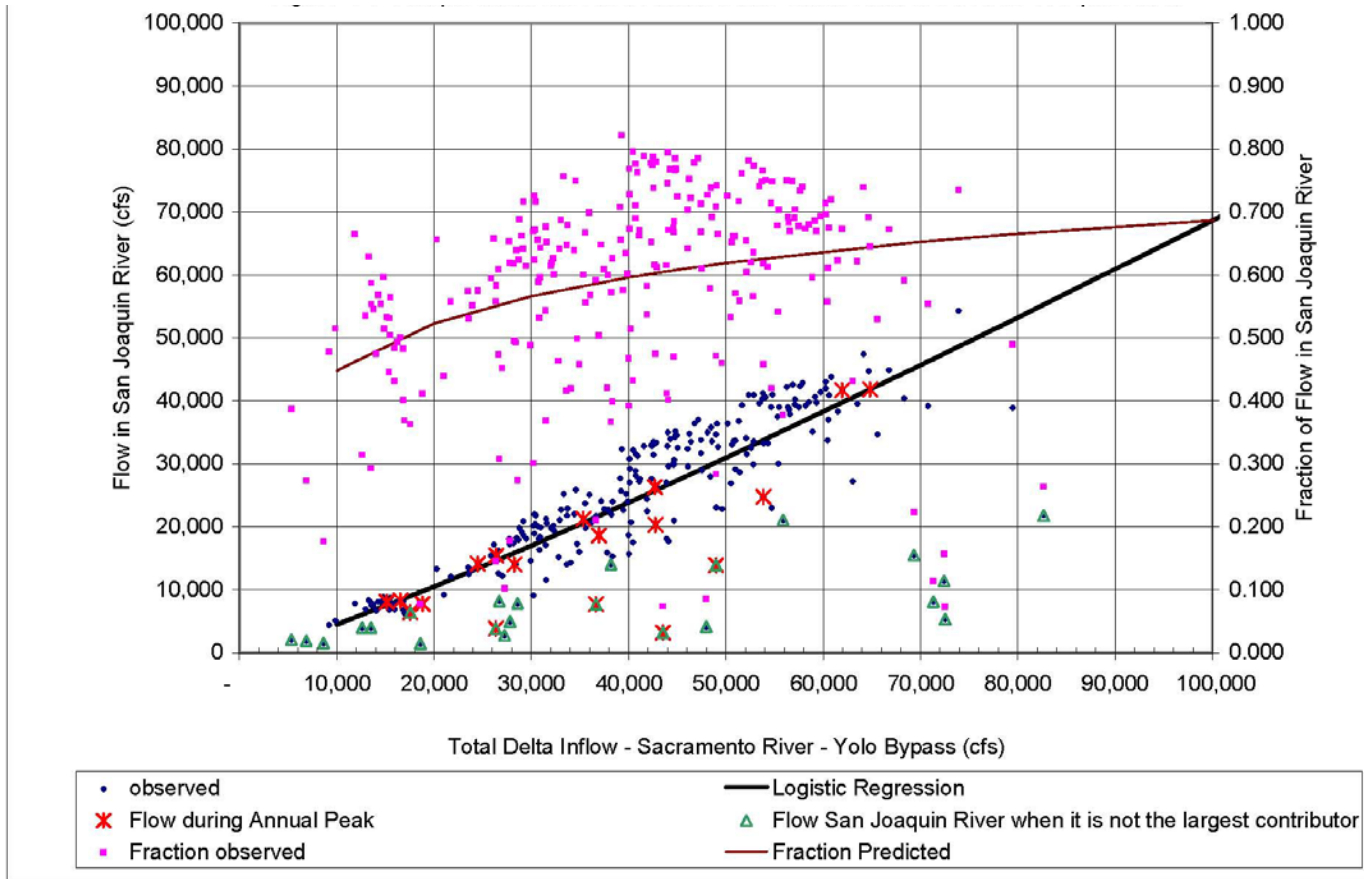


Figure 7-10 Comparison Between Predicted and Observed Flow in San Joaquin River

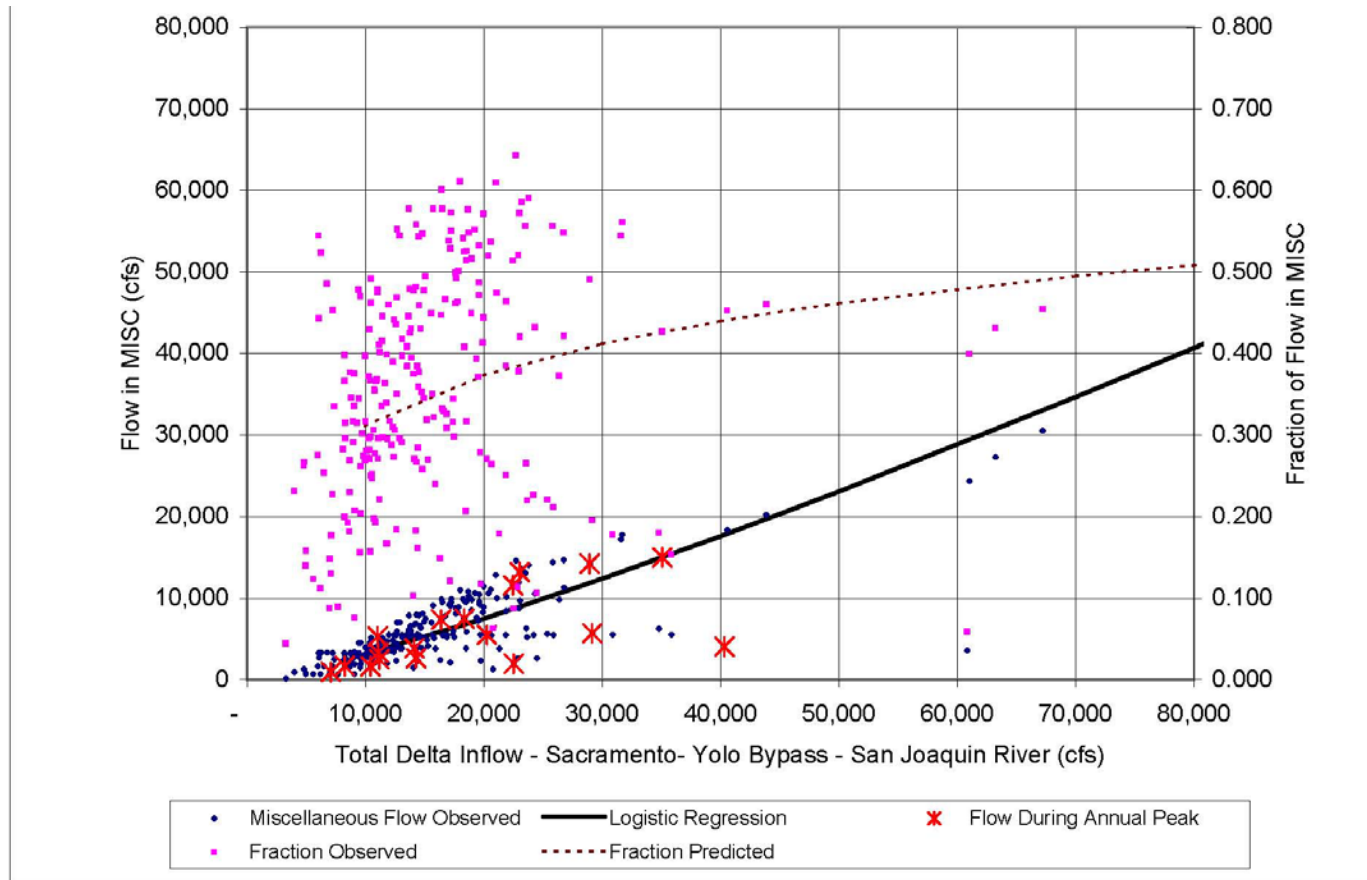


Figure 7-11 Comparison Between Predicted and Observed Flows in MISC Inflow

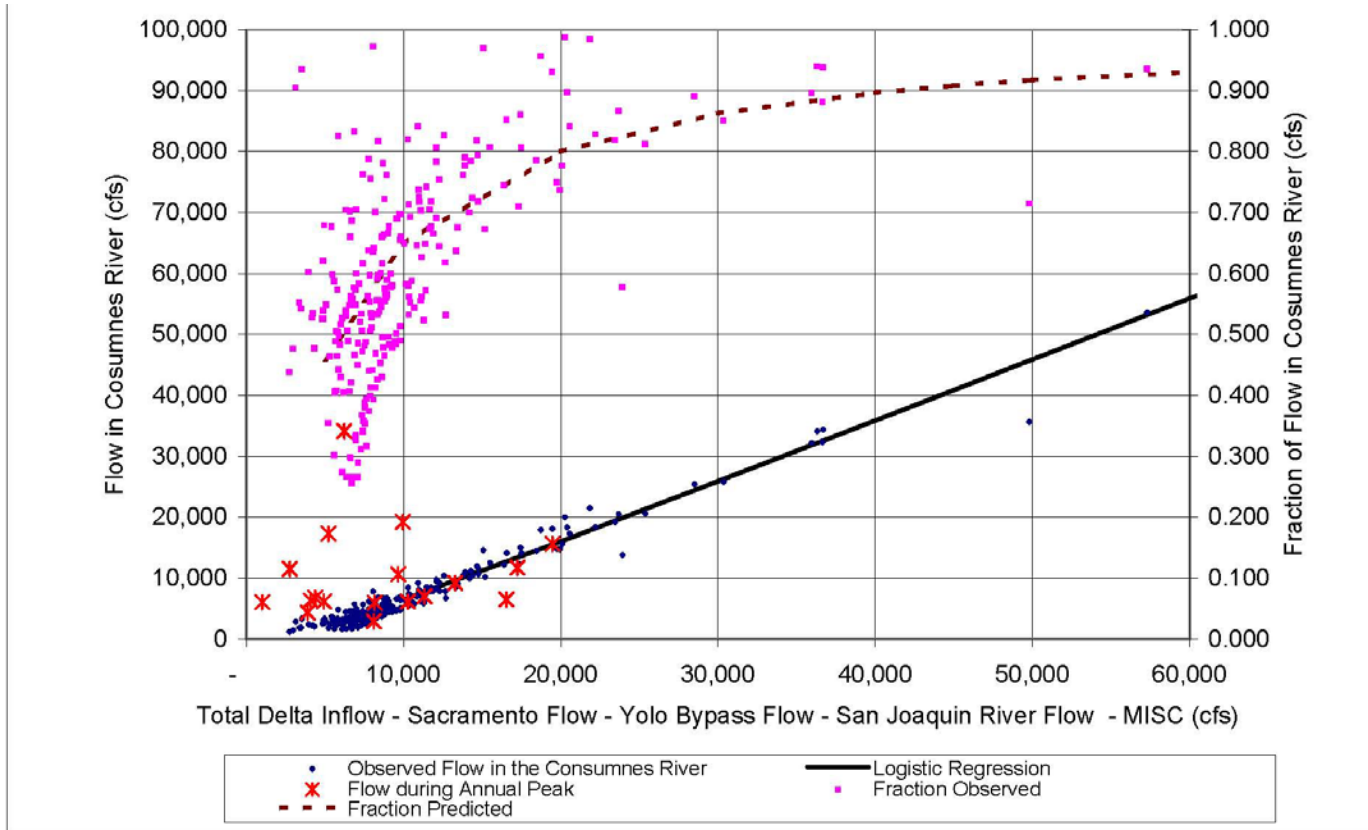


Figure 7-12 Comparison Between Predicted and Observed Flows in the Cosumnes River

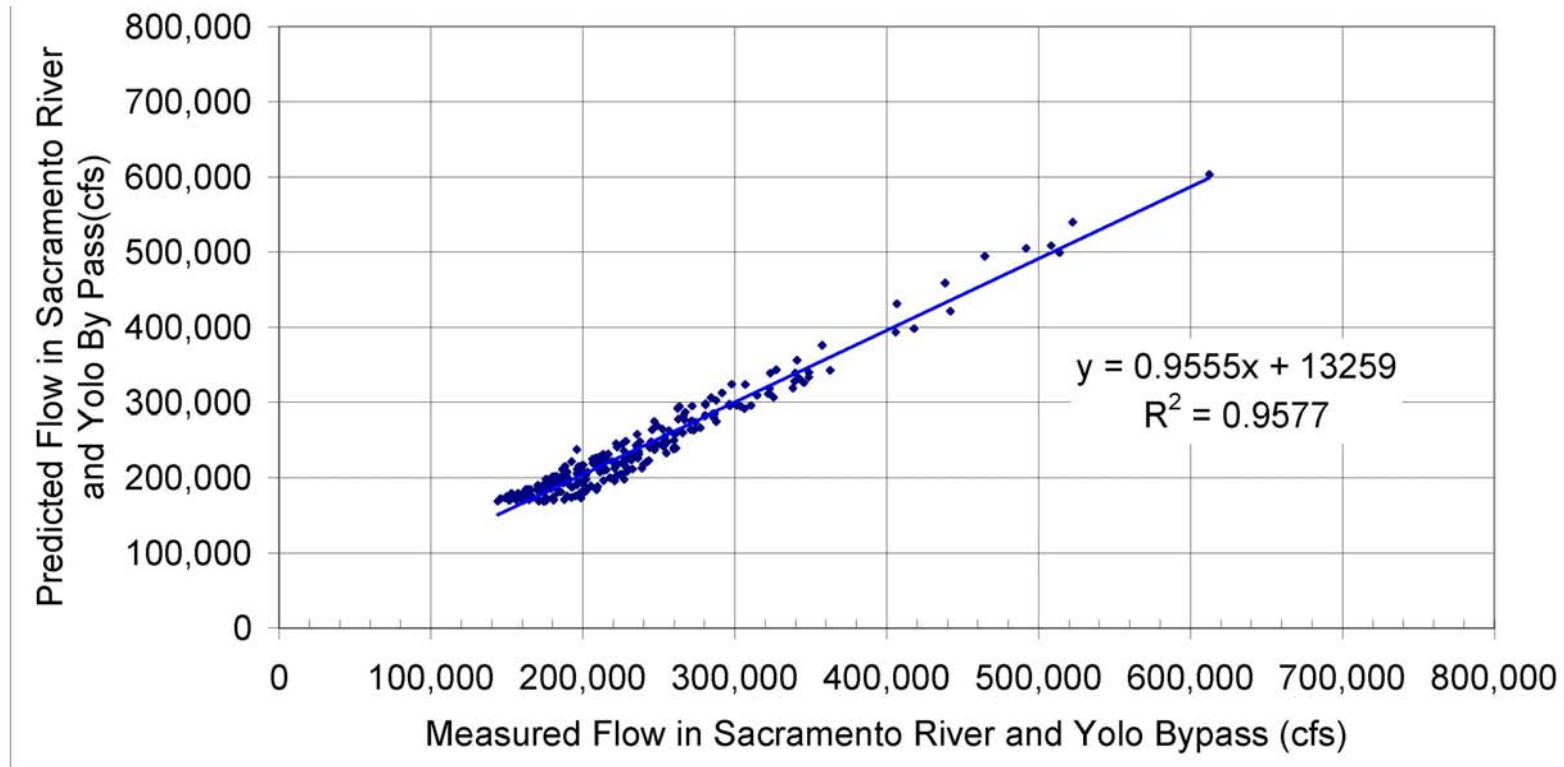


Figure 7-13 Comparison Between Measured and Predicted Flows in the Sacramento River and Yolo Bypass

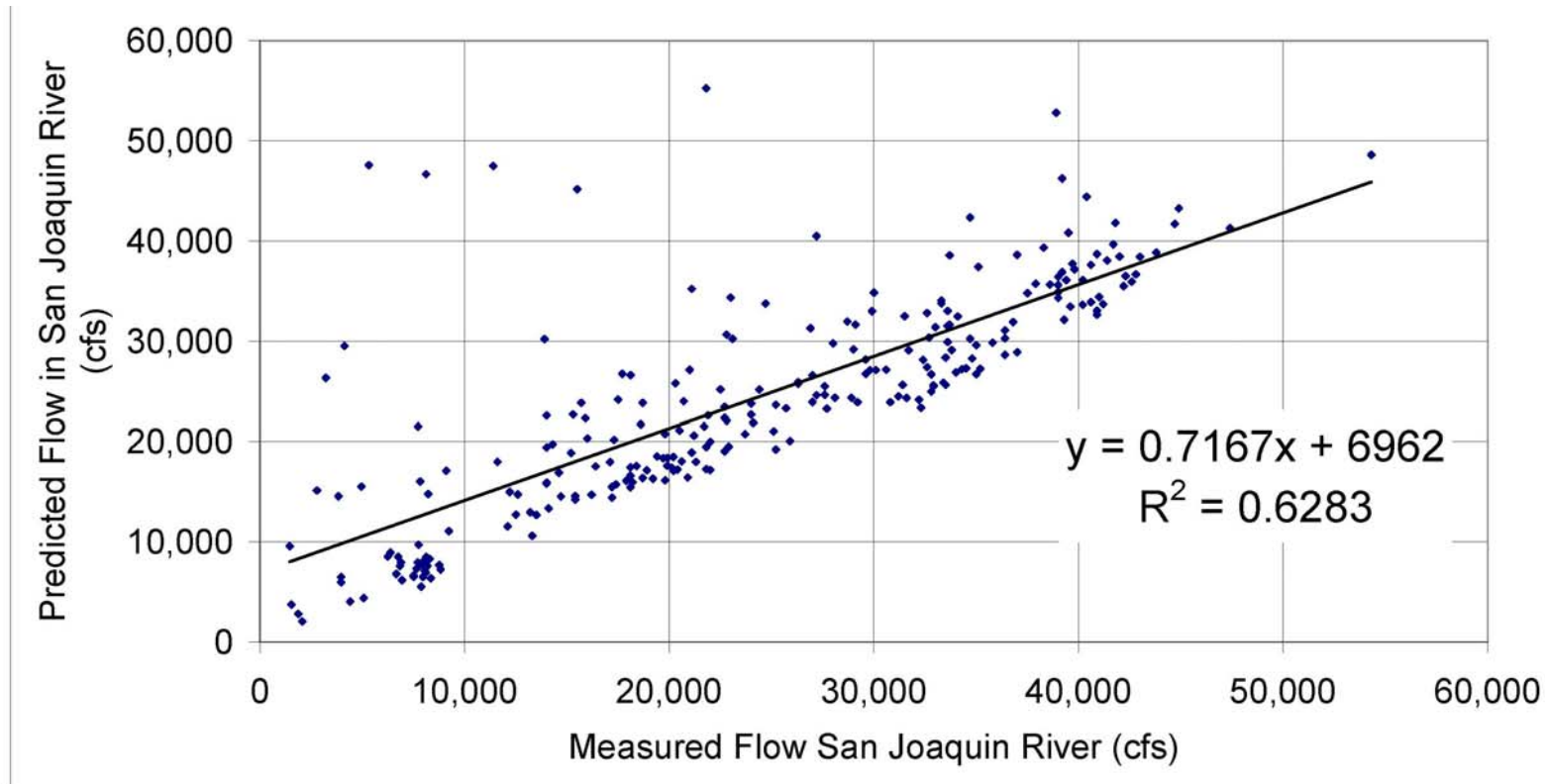


Figure 7-14 Comparison Between Measured and Predicted Flows in the San Joaquin River

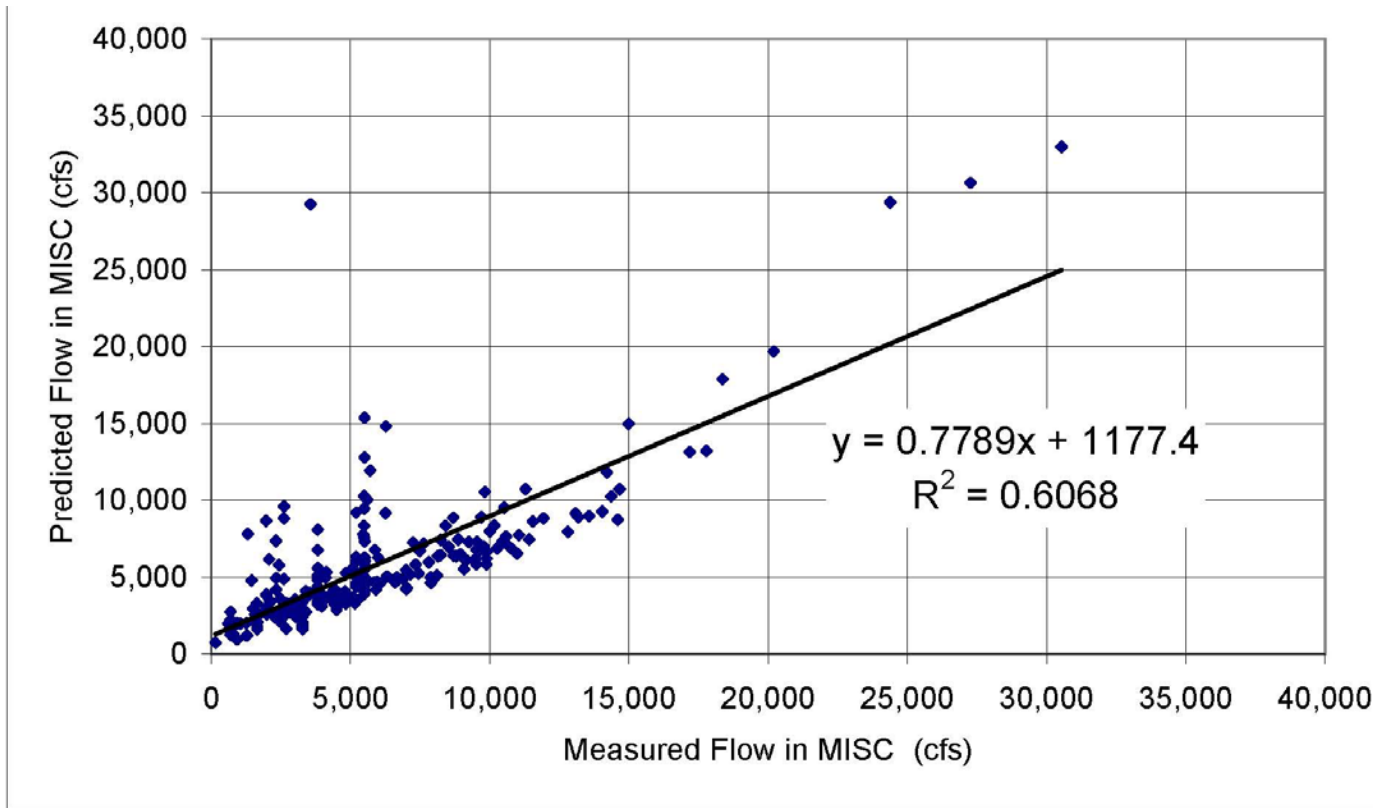


Figure 7-15 Comparison Between Predicted and Measured Flows in the Miscellaneous Inflows

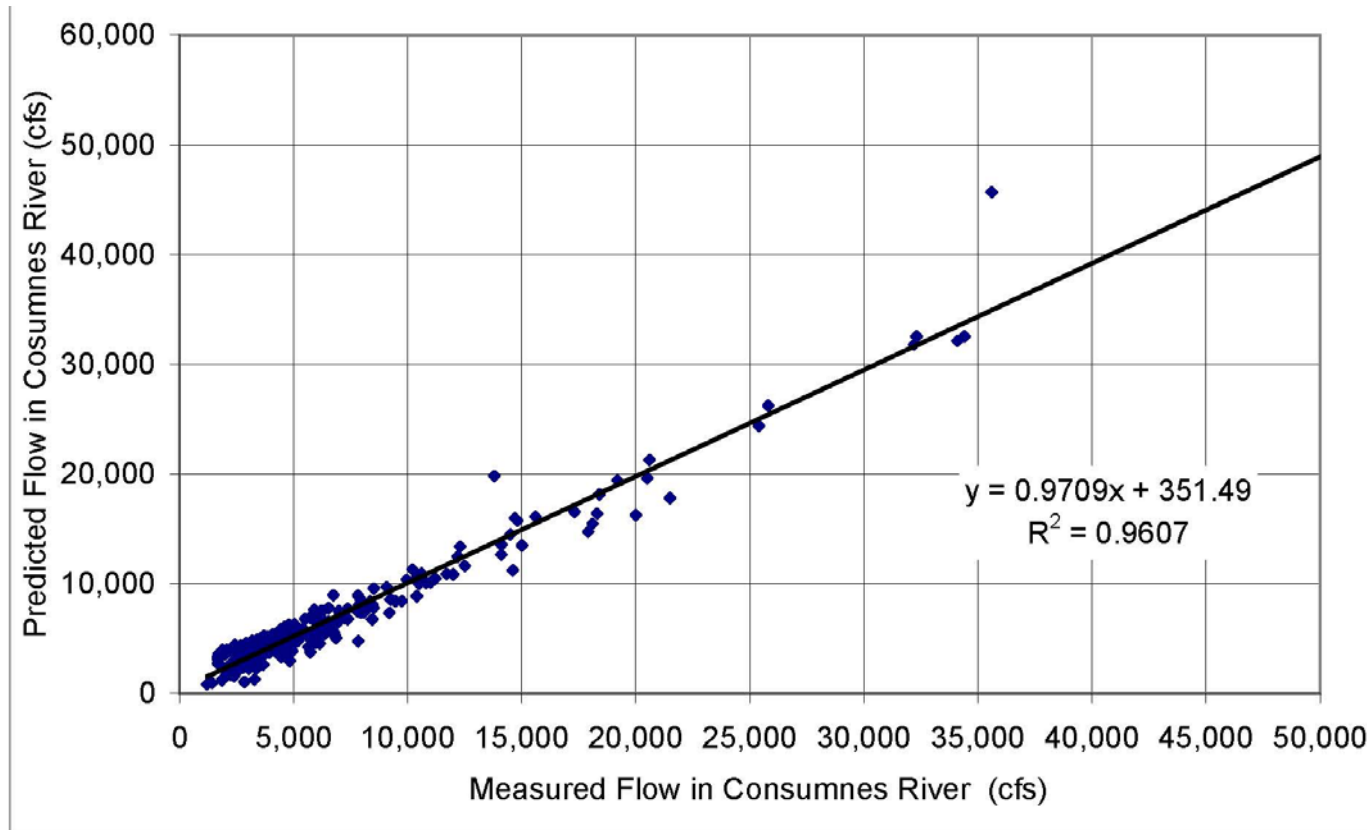
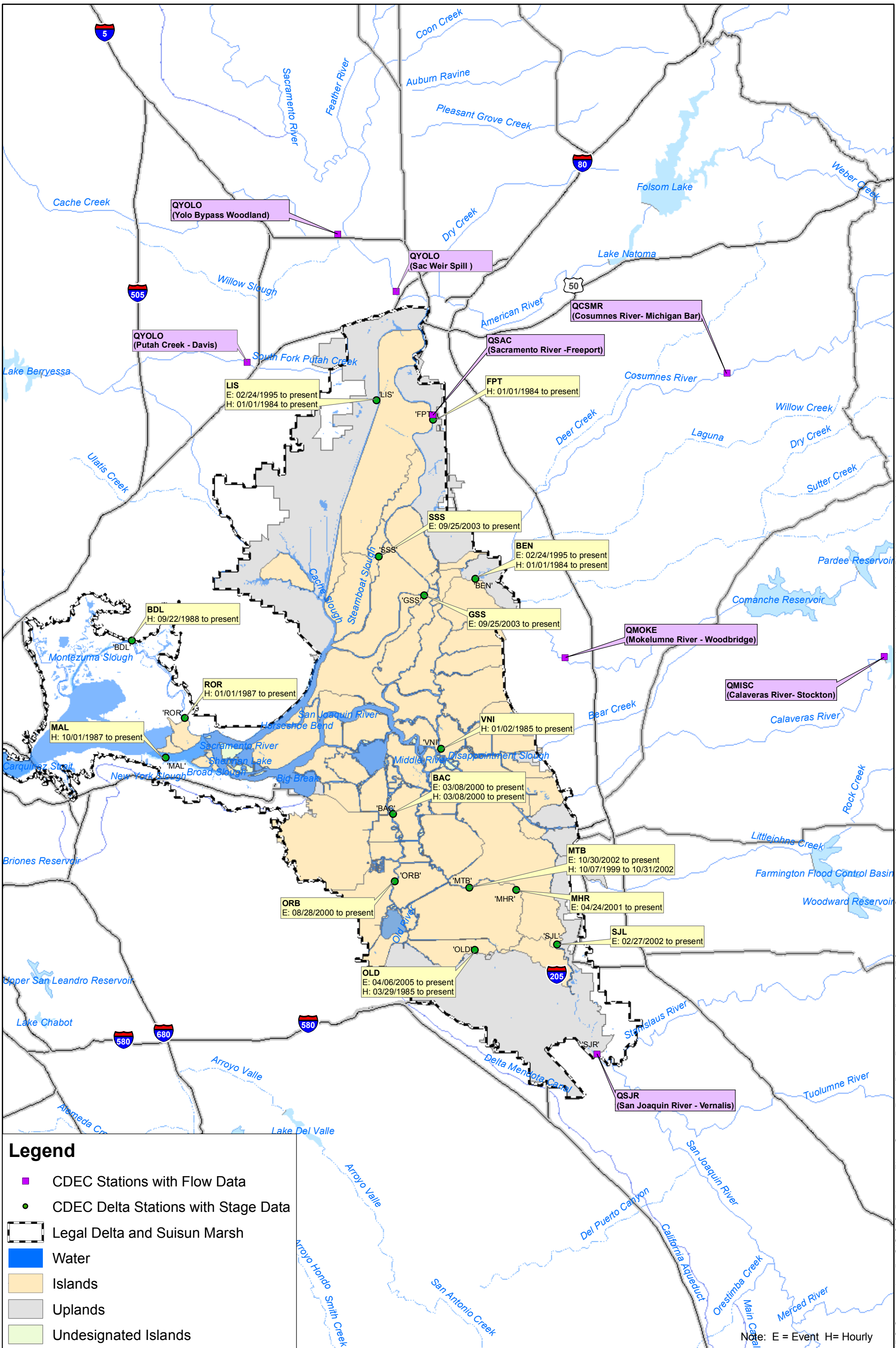


Figure 7-16 Comparison Between Predicted and Measured Flows in the Cosumnes River



Legend

- CDEC Stations with Flow Data
- CDEC Delta Stations with Stage Data
- ▭ Legal Delta and Suisun Marsh
- Water
- Islands
- Uplands
- Undesignated Islands

Note: E = Event H= Hourly

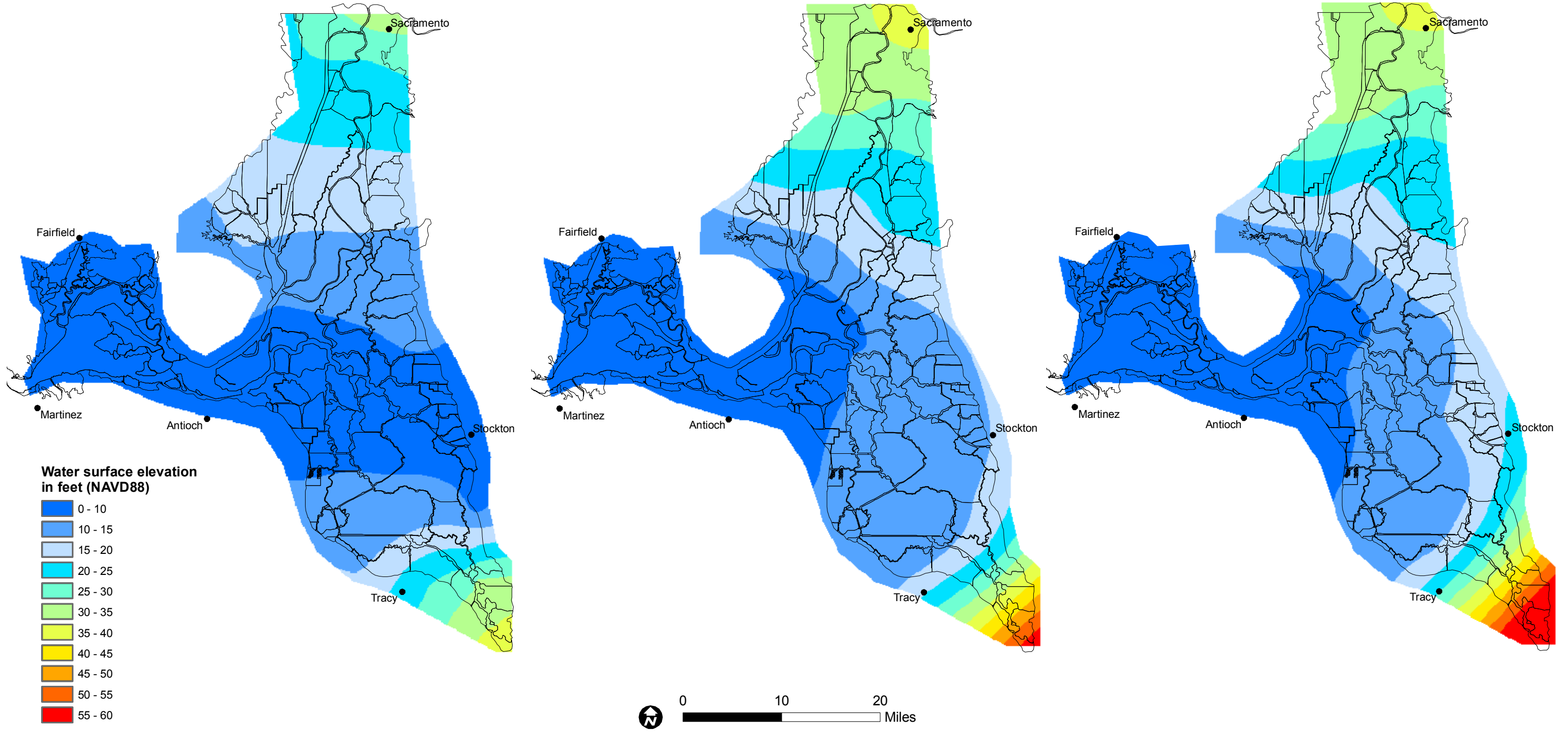


URS Corporation P:\GIS\GIS_Project_Files\OriginalData\Regional_Data\CDEC_stations_data\Regional_Data\CDEC_stations_data\used_for_regression_analyses.mxd Date: 12/14/2006 2:20:39 PM Name: smlewis0

FEMA 100-year
water surface elevations

Median water surface elevations
for median 100-year total Delta inflow

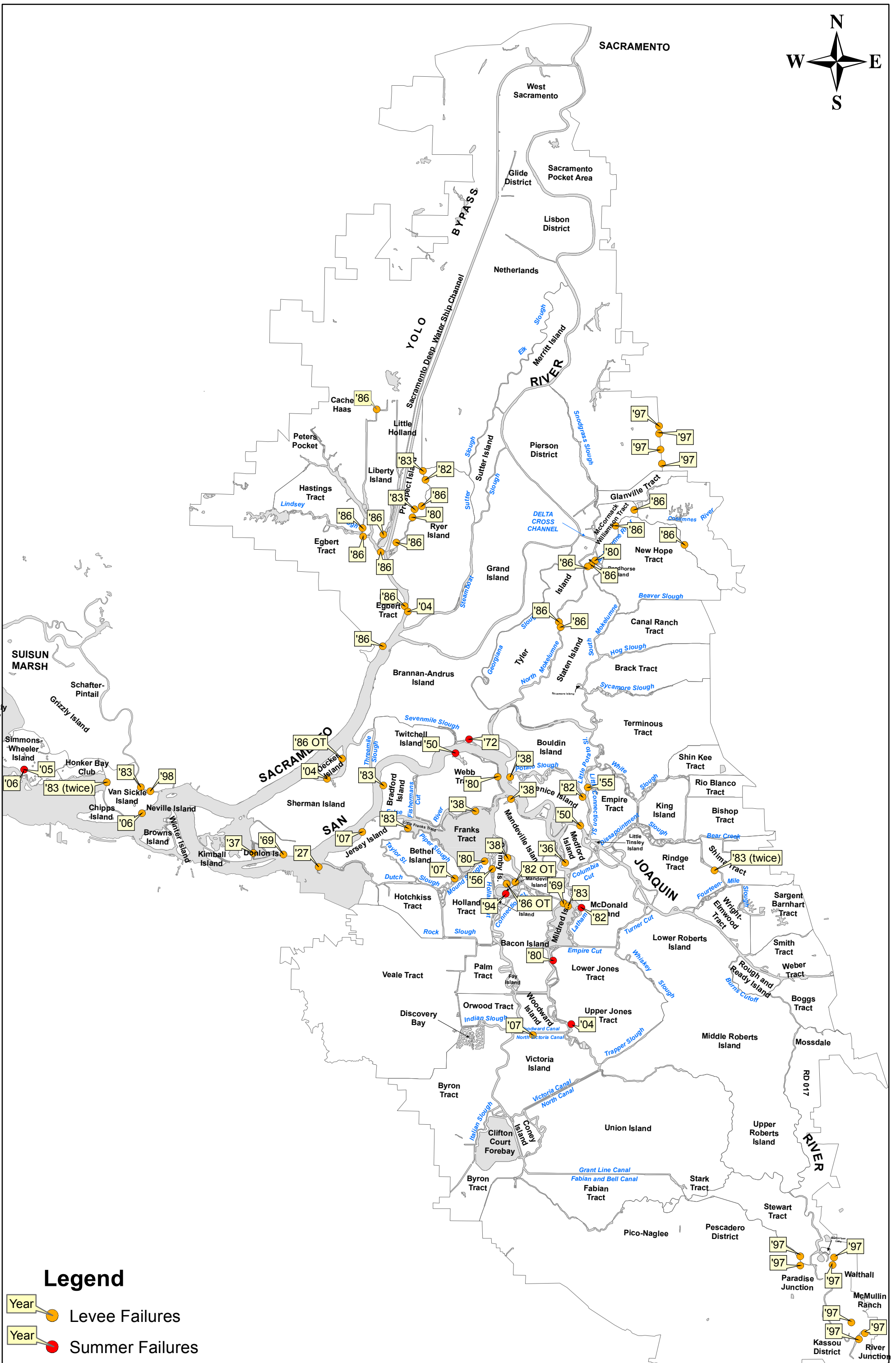
Median water surface elevations
for median 100-year total Delta inflow,
10% confidence level for Sacramento River inflow,
90% confidence level for San Joaquin River inflow



DRMS
26815431

100-year Flood Elevations
in the Delta

Figure
7-18



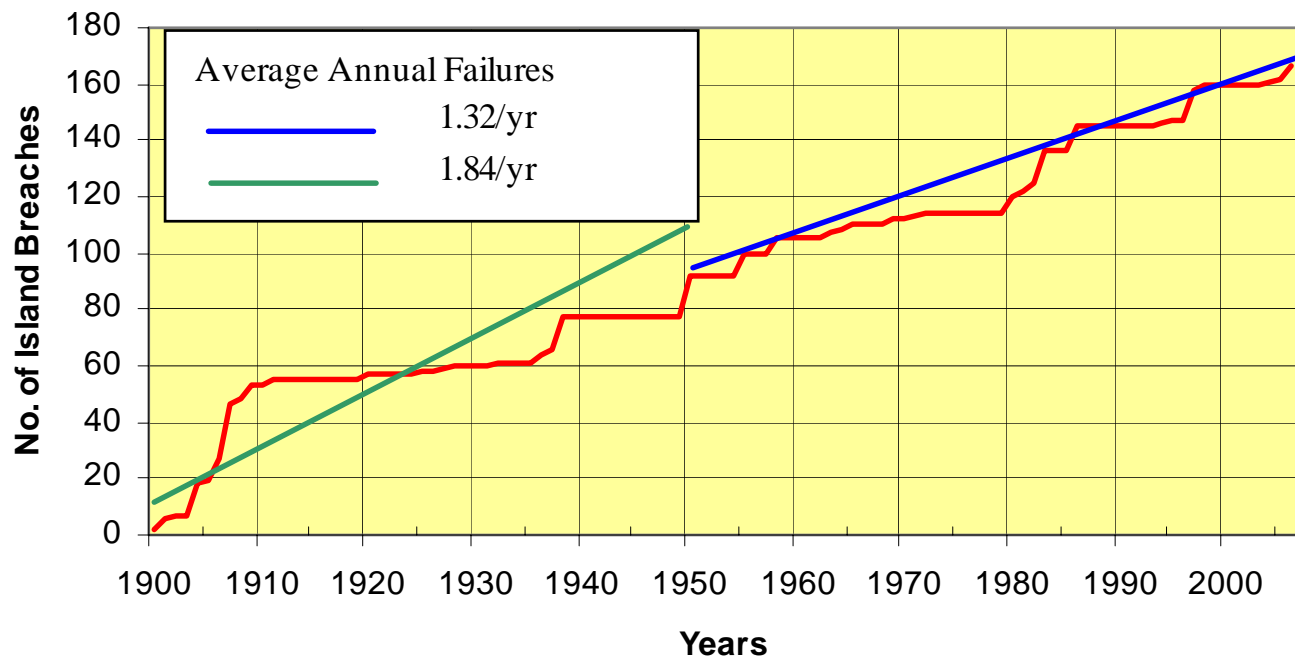
Legend

- Year ● Levee Failures
- Year ● Summer Failures



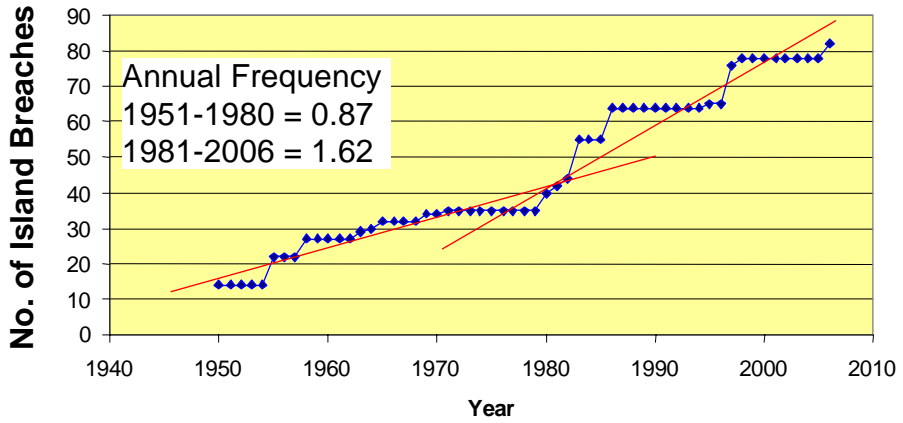
	DRMS	Locations of Levee Failures	Figure 7-20
	26815431		

URS Corporation P:\GIS\GIS_P\Project_Files\GIS\Analysis\Levee_Failure\Problem_Areas_Failure_Analysis\Levee_Failure_Analysis.mxd Date: 11/29/2006 2:44:25 PM Name: dhwerg0

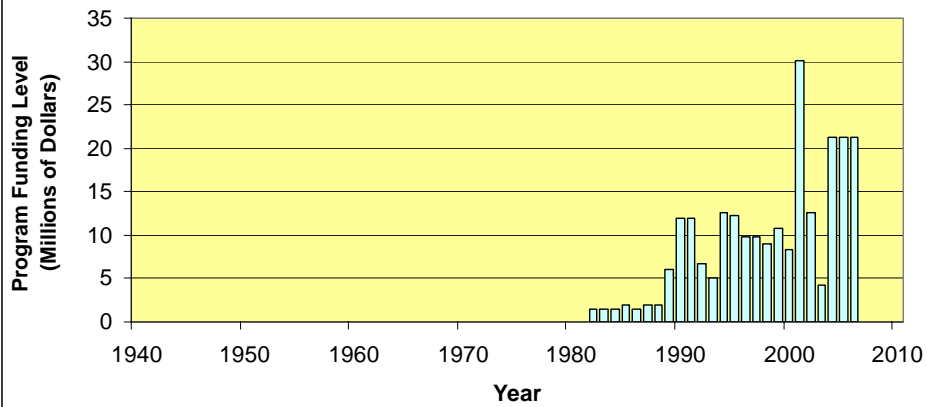


Delta Risk Management Strategy (DRMS) Levee Fragility		Cumulative Number of Island Breaches Since 1900	Figure 7-21
URS	Project No. 26815621		

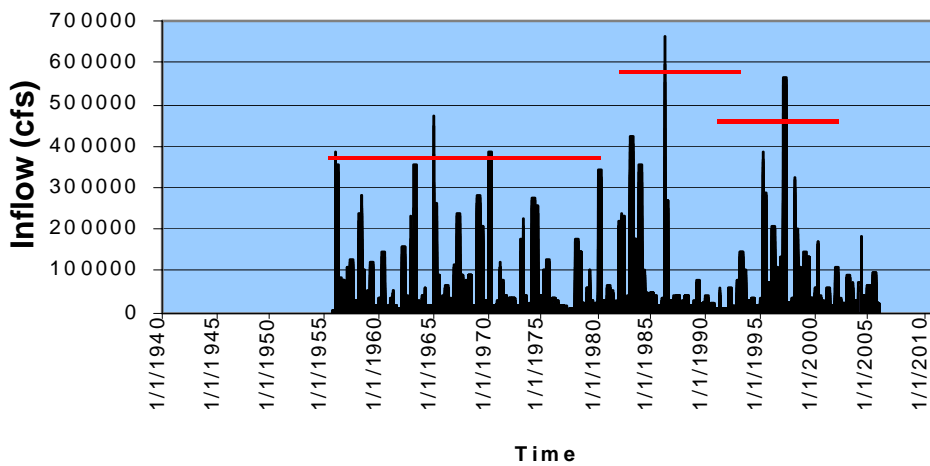
7-22(a) Cumulative Number of Flooded Islands

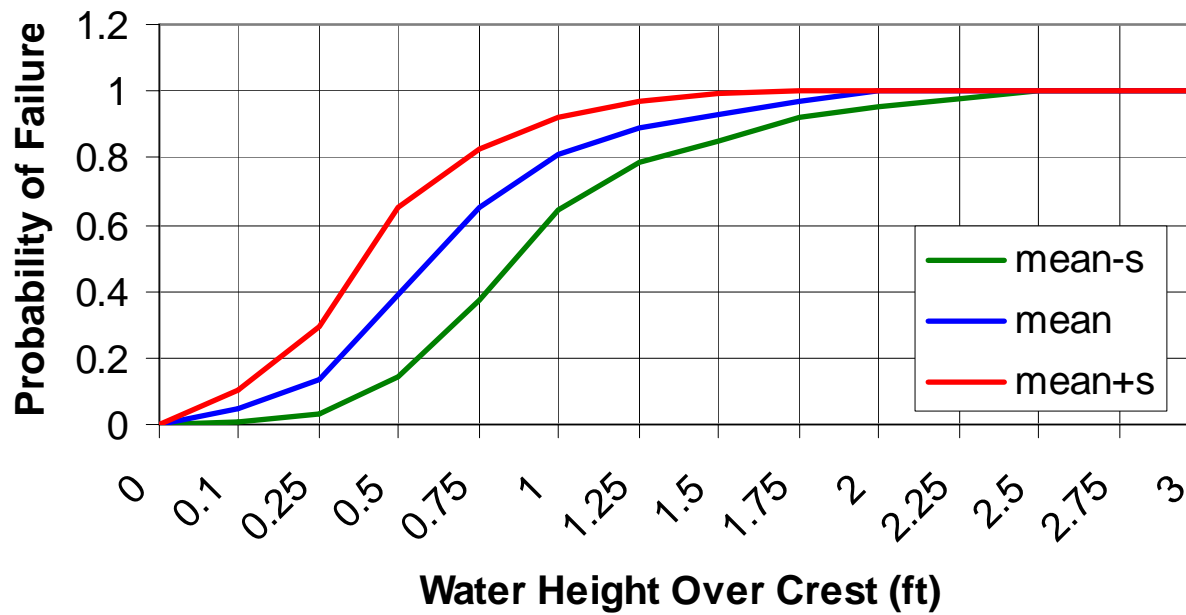


7-22(b) Program Funding Level



7-22(c) Total Inflows (cfs)





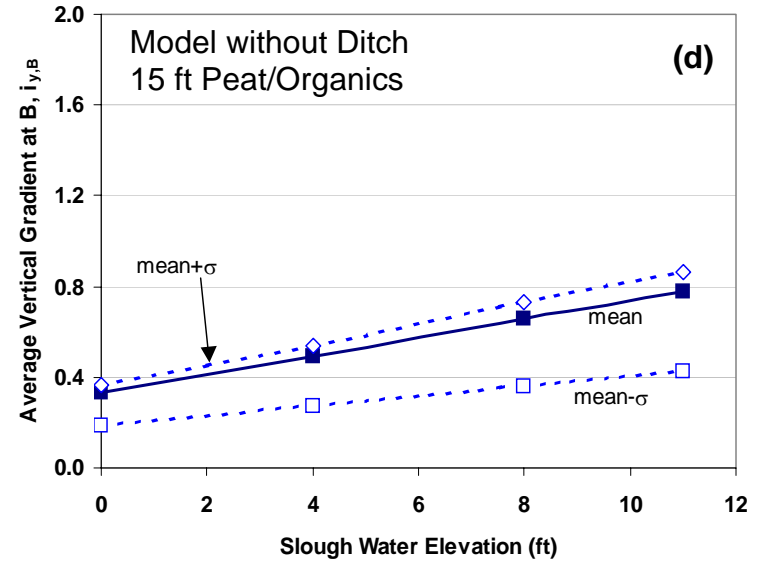
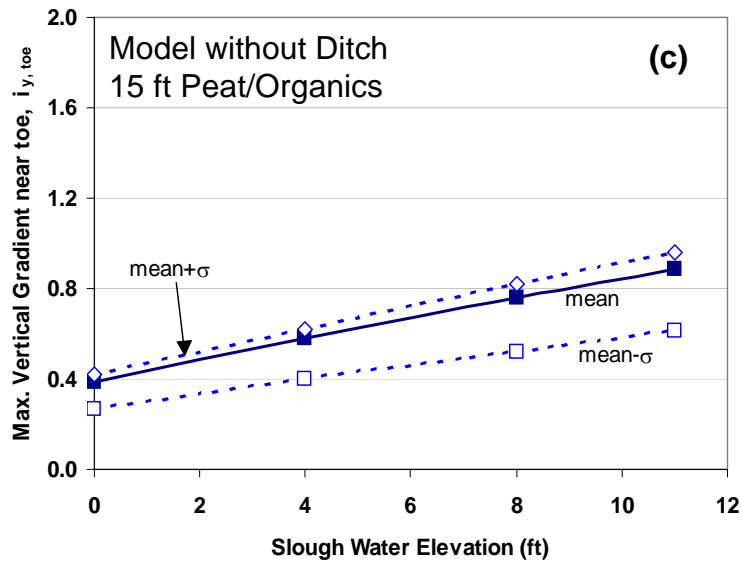
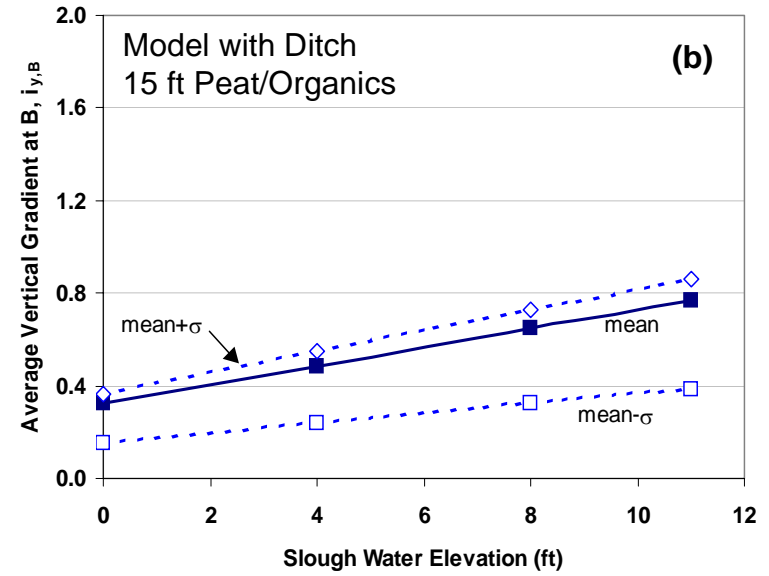
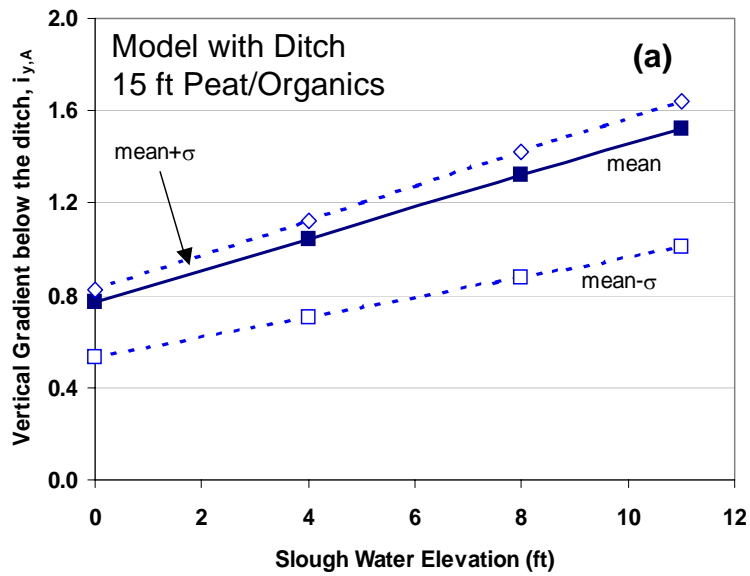
Delta Risk Management Strategy (DRMS)
Levee Fragility



Project No. 26815621

Probability of Failure versus
Water Height over the Crest -
Overtopping Failure Mode

Figure
7-23



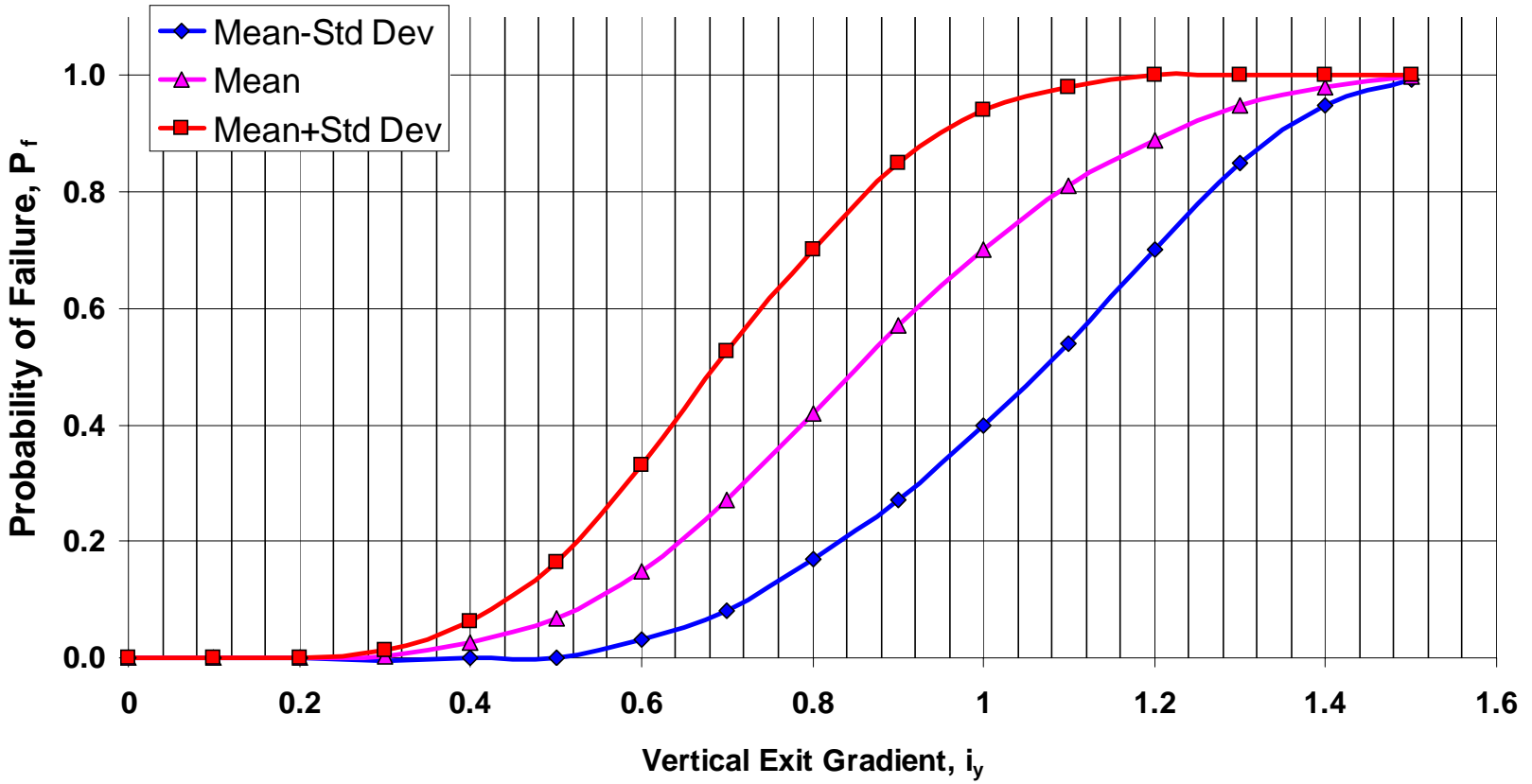
Note:
 Analysis model: Typical cross section for Delta with/without drainage ditch and without slough sediment, and for the case of not-narrow slough

Delta Risk Management Strategy (DRMS) Levee Fragility	
URS	Project No. 26815621

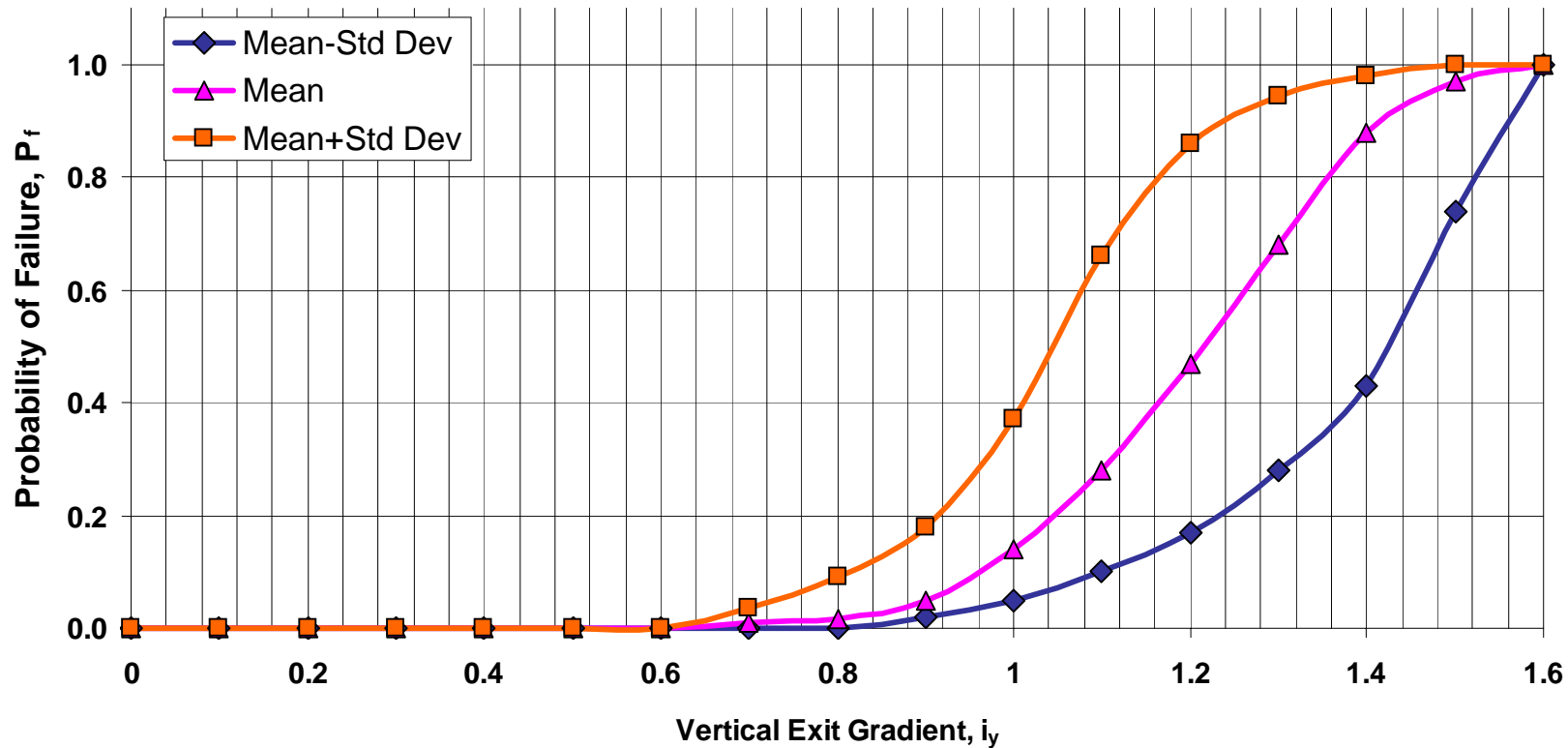
Computed Vertical Gradients
 for Typical Cross Sections with &
 without Ditch for 15 ft Peat/Organics

Figure
 7-24

Probability of Failure versus Vertical Exit Gradient for Under Seepage (smoothed)
 -No Human Intervention



Probability of Failure versus Vertical Exit Gradient for Under-seepage (Smoothed) -
With Human Intervention

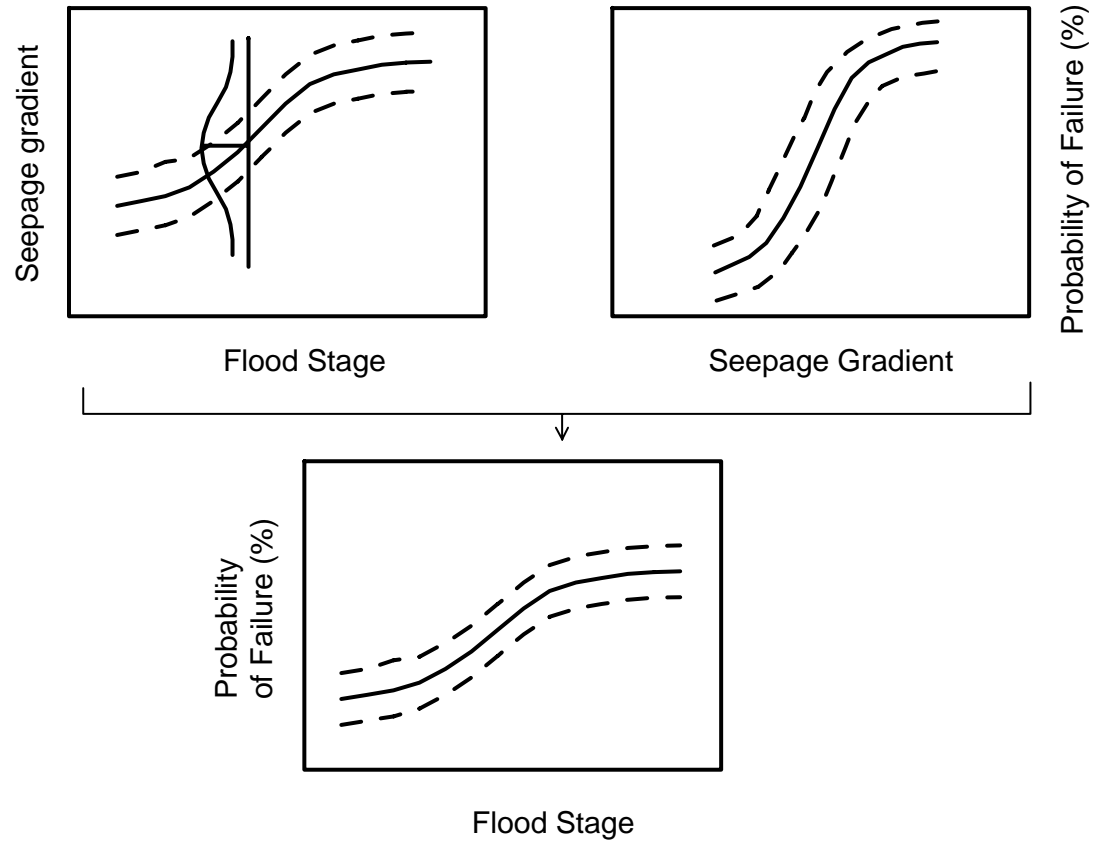


Delta Risk Management Strategy (DRMS) Levee Fragility	
URS	Project No. 26815621

Probability of Failure versus
Exit Gradient
- With Human Intervention

Figure
7-26

For Vulnerability Class i,



Delta Risk Management Strategy (DRMS) Levee Fragility		Probability of Failure versus Flood Stage	Figure 7-27
URS	Project No. 26815621		